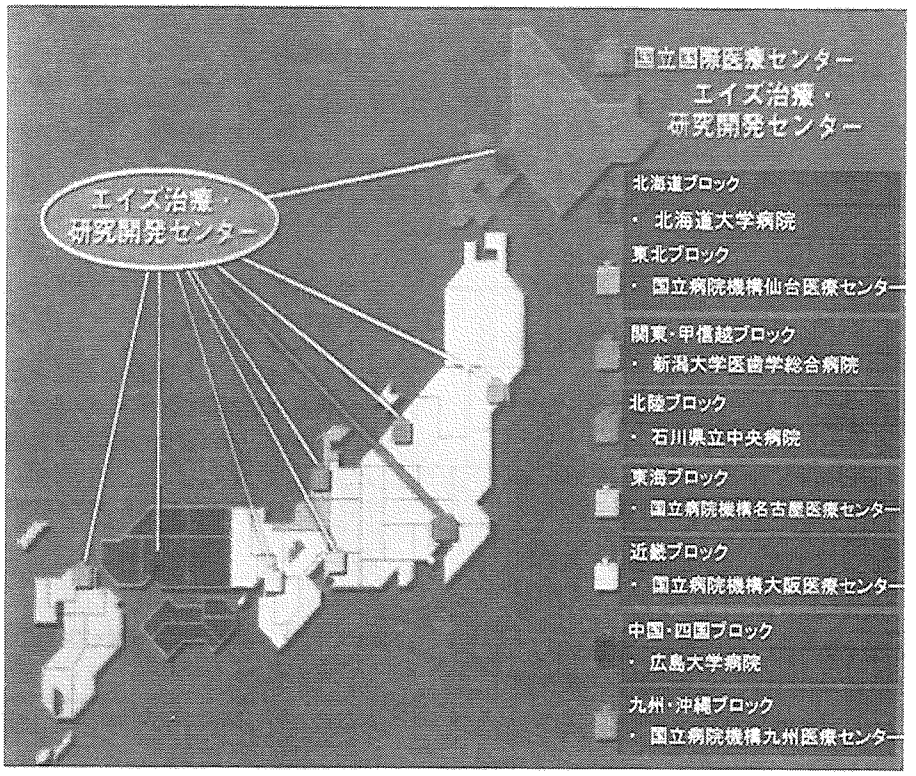

図11　エイズ医療体制診療ネットワーク

表10　地域エイズ拠点病院への提言（三間屋純一）

1) 常日頃より院内において医療従事者のHIVおよびエイズに対する正しい知識の教育と患者・感染者に対してソフト面での受け入れ体制を整備しておく
　　特に拠点病院においては必須である
2) 告知前カウンセリング
　　患者・感染者のHIVおよびエイズに対する認識度の把握を行う
3) 病名告知
　　患者・感染者の立場を理解した慎重なものでなければならない
　　告知後のフォローを円滑に進める為にも，出来ればナースやカウンセラーに同席してもらう
4) 患者・感染者に対しHIVおよびエイズに対する正しい医学知識と最新情報の提供を行う
5) 患者・感染者に本人の現在の病状を詳しく説明し，今後の治療方針を提示する
6) 告知後の診療面および心理面での支援体制の確立
　　院内各診療科へ出向き患者背景を説明し診療の協力を要請する
　　co-medicalへ精神面での援助とプライバシーの保護を依頼する
　　患者・感染者の希望があれば近医療機関や他の患者およびボランティア団体を紹介する

るためにはワクチンの開発が急務となる．現在世界では4千万人以上の人々がHIVとともに生活し，毎日1万4千人の人が新たに感染しているといわれている．現行の予防対策と治療プログラムを拡充することは当然であるが，同時に，新たな予防技術の開発を迫られている．その意味でも，予防ワクチンの開発こそが，エイズ流行とそれに付随する莫大な被害を食い止める，もっとも有効な長期的対策である．現在，30以上のワクチン候補が臨床試験に進んでいる．国際エイズワクチン推進構想(IAVI)は1996年に設立された国際的な非営利・非政府組織で，HIVの感染とエイズ発症を予防するワクチンの開発促進を目指して活動している．エイズワクチン開発には途上国との連携が重要で，IAVIはアフリカやアジアの研究者とともに，ウイル

表11　共同研究者

◆静岡県立こども病院
　血液腫瘍科
　　殿内力，豊田恭徳，堀越泰雄，高嶋能文，西尾信博，奈良妙美
　臨床病理科
　　杉山武喜子，山崎あけみ，薗田明弘，塚本道子，高原勝行
　指導相談室
　　紅林洋子，大久保俊夫
　薬剤部
　　鈴木崇代，坂本達一郎，鈴木貴也
　看護部
　　黒木久美子，河野芳子，平野友子，加藤富久子，土居泰子，高橋定子，富永智栄子
　歯科
　　加藤光剛，松浦芳子
◆静岡県立大学　薬学部
　　川端寛樹，内藤博敬，森田全
◆熊本大学医学部　第二内科
　　服部俊夫，高月清
◆東京医科大学　臨床病理科
　　池松正次郎，羽田雅夫，福武勝幸
◆聖マリアンナ医科大学　小児科
　　山田兼雄，目黒嵩，立浪忍，瀧正志
◆国立感染症研究所エイズ研究センター
　　中永和枝，吉原なみ子
◆山梨医科大学　微生物学
　　照沼裕，とう学文

（所属は研究当時）

スの異なるサブタイプの見られる途上国向けに，安全，効果的で安価に製造できるワクチン開発に向け研究を重ねている．日本の研究者もアフリカやタイの研究者と協力し，ワクチンの臨床試験を行っているところである．

おわりに―日本の役割

本年7月神戸で開かれた第7回アジア・太平洋地域エイズ会議[34)35)]の場で，国際社会より，このまま日本は沈黙をまもり，本国におけるHIV感染拡大の防止の必要性の事実をひたすら覆い隠し，近い将来くるであろう感染爆発を見守るのか？と危惧されている．この指摘に対し，これまで以上に積極的予防対策を講じ，国民ひとり，ひとりがこのエイズ問題を自分自身の問題として真剣に考える時期にきているのではないだろうか．また，本会議でUNAIDSの事務局長Peter Piot氏は日本のAIDS対策として，先ず国内のエイズ予防策を強化し，教育を徹底し，エイズ問題をオープンに話せる環境造りが最も大切であると提言している．また同時にアジアで唯一のG8の一員である日本はエイズ問題においても世界的なリーダーシップ，特に財政支援の面での役割を担うことを期待しているとのコメントがなされている．この点に関しては，本年6月に東京で開催された世界エイズ・結核・マラリア対策基金のシンポジウムにおいて小泉首相は，基金に対して従来の3.27億米ドルに加え，新たに5億米ドルの追加資金の拠出を誓約している．このような資金面での国際貢献は非常に大切なことであるが，世界は一つの共同体であることを認識し，エイズが人間の尊厳に関わる問題であり，社会の根源に関わる重大な問題であり，さらに世界各地での流行拡大が日本にも影響を及ぼすという認識を持ち，先ず第1に自分たち日本人自身の足元を固める事を最優先しなければならない．その為には行政，医療機関，マスコミ，NGOなどの民間団体がタッグを組んで再度対策を見なおすべきであろう．

文　献

1) 三間屋純一，福武勝幸，西田恭治，他．HIV感染症と血友病―回顧と展望―．日本エイズ学会誌　2005；7：61―76.
2) 三間屋純一．会長講演「1982年より臨床現場においてエイズ診療と研究を通して感じたこと」．日本エイズ学会誌　2004；6：75―77.
3) 殿内　力，小島勢二，三間屋純一，他．血友病と免疫異常．小児科　1984；25：177―180.
4) 三間屋純一，殿内　力，豊田恭徳，他．静岡県下における血友病患者のHTLV-III汚染時期に関する検討．医学のあゆみ　1985；135：573―574.

5) Mimaya J, et al. Retrospective study of seropositivity of HIV and immunity of Japanese Hemophiliacs. Pro 5th Int Symp 1986；265—274.
6) 堀越泰雄，市川正孝，殿内　力，他．HIV 感染血友病患者における DNA-PCR および RT-PCR 法によるプロウイルスおよびゲノム RNA の検出．臨床血液　1993；34：620—627.
7) Morita T, Kawabata K, Mimaya J, et al. Time-course detection of HIV-1 proviral DNA and genomic RNA by polymerase chain reaction in sera from seropositive and seronegative hemophiliacs treated with clotting factor concentrates. Int J Hemat 1993；8：225—232.
8) 三間屋純一，他．AIDS および関連疾患—感染から発症までの臨床経過．病理と臨床　1993；11：331—342.
9) 三間屋純一．HIV 感染症の病態と臨床—臨床経過と追跡マーカー—．臨床血液　1995；36：424—434.
10) 三間屋純一．血友病と HIV 感染の現状．医学のあゆみ　1996；176：7—11.
11) Naito H, Mimaya J, Horikoshi Y, et al. Quantitative Defection of HIV-1 RNA by PCR and Use as a Prognostic Marker and for Evaluating Antiretroviral Therapy. Biol Pharm Bull 1997；20：1317—1320.
12) 三間屋純一．AIDS の治療—長期未発症例．臨床科学　1997；33：43—48.
13) 三間屋純一．HIV 感染における Long-term non-progressor．血液・免疫・腫瘍　1998；3：41—48.
14) 三間屋純一，目黒　嵩，根岸昌功，他．National History 委員会報告—長期未発症例の実態調査結果と CD4 200cells/μl 以下の症例の予後を中心に—厚生省平成 7 年度 HIV 感染者発症予防・治療に関する研究班報告書．1995.
15) 三間屋純一，目黒　嵩，立浪　忍，他．HIV 感染者の長期予後に関するコホート研究．厚生省 HIV 感染者発症予防・治療に関する研究班．平成元年度研究報告書．1989：13—23.
16) 三間屋純一，目黒　嵩，立浪　忍，他．Natural History 委員会研究報告．厚生省 HIV 感染者発症予防・治療に関する研究班．平成 2 年度研究報告書．1990：9—16.
17) 三間屋純一，目黒　嵩，立浪　忍，他．Natural History 委員会研究報告．厚生省 HIV 感染者発症予防・治療に関する研究班．平成 3 年度研究報告書．1991：9—16.
18) 三間屋純一，目黒　嵩，立浪　忍，他．Natural History 委員会研究報告．厚生省 HIV 感染者発症予防・治療に関する研究班．平成 4 年度研究報告書．1992：9—16.
19) 三間屋純一，目黒　嵩，立浪　忍，他．Natural History 委員会研究報告．厚生省 HIV 感染者発症予防・治療に関する研究班．平成 5 年度研究報告書．1994：37—45.
20) 血液凝固異常症全国調査運営委員会（瀧　正志，立浪　忍，白幡　聡，三間屋純一，他）．血液凝固異常症全国調査．平成 16 年度報告書．1995 年 4 月.
21) 2004 年（平成 16 年）エイズ発生動向年報．厚生労働省エイズ動向委員会．平成 17 年 4 月 25 日.
22) 三間屋純一，他．HIV-1 感染血友病患者における HIV-1 抗原（p24）と HIV-1 抗体（gp41，p24）の経時的観察．臨床血液　1988；29：795—801.
23) 三間屋純一，他．感染から発症までの臨床経過．病理と臨床・臨時増刊号　1993；11：331—342.
24) 三間屋純一，他．HIV 感染症・AIDS．血中 P24 抗原検出法．日本臨床　1993；51：211—224.
25) 森田　全，他．HIV 感染症・AIDS．血中 HIV-RNA 検出法．日本臨床　1993；51：284—289.
26) 堀越泰雄，三間屋純一，他．HIV 感染症・AIDS．感染細胞におけるプロウイルス DNA の検出法．日本臨床　1993；51：290—298.
27) 高嶋能文，三間屋純一，他．HIV 患者・感染者に対するプロテアーゼ阻害剤を含む抗 HIV 剤多剤併用療法の効果—長期投与例も含めて—．臨床とウイルス　1998；26：24—31.
28) HIV 感染症治療研究会（木村　哲，満屋裕明）．HIV 感染症『治療の手引き』第 8 版，2004 年 12 月．http://www.hivjp.org/
29) 中村哲也，他．抗 HIV 治療ガイドライン　平成 16 年度研究報告書—厚生労働科学研究費補助金エイズ対策研究事業省．HIV 感染症の医療体制に関する研究班．2005 年 3 月.
30) 白阪琢磨，他．多剤併用療法服薬の精神的，身体的負担軽減のための研究班　平成 16 年度研究報告書—厚生労働科学研究費補助金エイズ対策研究事業．2005 年 3 月.
31) 高嶋能文，三間屋純一，他．d4T，3TC，内服中に buffalo hump を認めた HIV 感染血友病の一例．日本エイズ学会誌　2000；2：8—14.
32) 三間屋純一．総説—小児の HIV 感染症．日小血会誌　1997；9：135—146.
33) Working Group on Antiretroviral Therapy. National Pediatric HIV Resource Center, Guidelines for the Use of Antiretroviral Agents in Pediatric HIV Infection；March 24, 2005.
34) 木村　哲，他．HIV 感染症の医療体制の整備に関する研究．平成 16 年度研究報告書—厚生労働科学研究費補助金エイズ対策研究事業．2005 年 3 月.
35) 7th ICAAP News：Friday 1～Monday 4, July 2005, Kobe.

Available online at www.sciencedirect.com
SCIENCE DIRECT®
ELSEVIER
Biochemical and Biophysical Research Communications 338 (2005) 1890–1896
BBRC
www.elsevier.com/locate/ybbrc

CD24 is expressed specifically in the nucleus pulposus of intervertebral discs

Nobuyuki Fujita [a,b,1], Takeshi Miyamoto [a,b,*,1], Jun-ichi Imai [c], Naobumi Hosogane [a,b], Toru Suzuki [a,b], Mitsuru Yagi [a,b], Kozo Morita [a,b], Ken Ninomiya [a,b], Kana Miyamoto [a,d], Hironari Takaishi [b], Morio Matsumoto [b], Hideo Morioka [b], Hiroo Yabe [b], Kazuhiro Chiba [b], Shinya Watanabe [c], Yoshiaki Toyama [b], Toshio Suda [a,*]

[a] *Department of Cell Differentiation, The Sakaguchi Laboratory, Japan*
[b] *Department of Orthopedic Surgery, Keio University School of Medicine, 35 Shinanomachi, Shinjuku-ku, Tokyo 160-8582, Japan*
[c] *Department of Clinical Informatics, Tokyo Medical and Dental University, 1-5-45 Yushima, Bunkyo-ku, Tokyo 113-8519, Japan*
[d] *Department of Medicine and Biosystemic Science, Graduate School of Medicine, Kyushu University, 3-1-1 Maidashi, Fukuoka 812-8582, Japan*

Received 8 October 2005
Available online 10 November 2005

Abstract

Intervertebral disc (IVD) consists of a soft gelatinous material in its center, the nucleus pulposus (NP), bounded peripherally by fibrocartilage, annulus fibrosus (AF). Despite the number of patients with IVD degeneration, gene expression analysis has not been undertaken in NP and therefore little is known about the molecular markers expressed in NP. Here, we undertook a microarray screen in NP with the other nine tissues to identify the specific cell surface markers for NP. Five membrane associating molecules out of 10,490 genes were identified as highly expressing genes in NP compared with the other tissues. Among them, we identified CD24, a glycosylphosphatidylinositol (GPI) anchor protein as a cell surface marker for NP. CD24 expression was also detected in the herniated NP and chordoma, a malignant primary tumor derived from notochordal cells, while it was absent in chondrosarcoma. Therefore, CD24 is a molecular marker for NP as well as the diseases of IVD.

Keywords: Intervertebral disc; Nucleus pulposus; CD24

Intervertebral disc (IVD) degeneration and concomitant herniation are the distinguishing anatomical features associated with lumbar disc disease (LDD). The molecular mechanisms leading to the onset of IVD degeneration are not well understood. Recent genetic studies in humans and mice indicate that genetic factors play an important role in the etiology and pathogenesis associated with LDD [1–3].

The IVD is composed of two discrete components termed the nucleus pulposus (NP) and the annulus fibrosus (AF). The interior structure, NP, is a soft gelatinous avascular cartilage-like tissue, derived from notochord, containing extracellular matrix proteins (ECM) rich in large proteoglycans such as aggrecan and collagens. ECM proteins play a central role in chondrocyte metabolism through regulation of growth factors and appear to be crucial for maintaining IVD homeostasis and integrity [4,5]. A recent genetic study demonstrated the role of cartilage intermediate layer protein (CILP), an ECM that acts as a modulator of LDD susceptibility through deregulation of TGFβ signaling [3].

The AF, a fibrous cartilage composed of an inner and outer coaxial lamella, is bound to the periphery of the NP. The onset of degenerative disc disease is marked by mechanical stress-induced apoptosis in the AF resulting

* Corresponding authors. Fax: +81 3 5363 3475.
E-mail addresses: miyamoto@sc.itc.keio.ac.jp (T. Miyamoto), sudato@sc.itc.keio.ac.jp (T. Suda).
[1] These authors contributed equally to this work.

0006-291X/$ - see front matter © 2005 Elsevier Inc. All rights reserved.
doi:10.1016/j.bbrc.2005.10.166

in degeneration and disruption of the outer disc tissue leading to herniation of the NP [6]. This sequelae of events is consistent with the susceptibility to LDD associated with aggrecan and collagen mutations that compromise the response of IVD cells to injury [1,2].

To further delineate the mechanism of NP function in IVD degeneration, we performed a microarray screening and cluster analysis to identify cell factors that were expressed specifically in NP tissue. Based on previous findings about the properties and function of NP cells, we screened several different tissues for comparison in our microarray analysis. These tissues include: avascular tissues such as AF and tendon, mesenchymal tissues such as skeletal muscle, skin, bone, AF, and tendon; and neurogenic tissues including spinal cord and brain. We found that expression of a heat-stable antigen termed CD24, a glycosylphosphatidylinositol-anchored cell surface protein, was upregulated in NP cells in a tissue specific manner.

CD24 is expressed in neurons, preB cells, T cells, and several cancer cells [7–10]. It also functions in differentiation and activation of granulocytes and B lymphocytes [11]. CD24 deficient mice show no gross physical or behavioral abnormalities, however the homeostatic proliferation of CD24 deficient T cells is reduced indicating that CD24 may be involved in cell proliferation [12].

In this study, we found that CD24 was high in NP and was detected in herniated NP tissue. We also determined CD24 expression was upregulated in chordoma, a malignant primary tumor derived from notochord cells. In contrast, we were unable to detect CD24 expression in chondrosarcoma, malignant tumors derived from mesenchymal cells.

Materials and methods

Microarray analysis. Total RNA was extracted and pooled from 10 different tissues including NP, AF, tendon, skeletal muscle, spinal cord, brain, skin, bone, bone marrow, and peripheral blood of 8-week-old male Wistar rats using TRIzol Reagent (Qiagen GmbH, Hilden, Germany). To ensure a sufficient amount of Poly(A)$^+$ RNA for screening, we pooled NP, AF, and tendon tissue from 50 rats. For the remaining tissues, we pooled tissue from 10 rats. Synthetic polynucleotides (80-mers) representing 11,464 rat transcripts derived from 10,490 independent genes (MicroDiagnostic, Tokyo, Japan) were arrayed with a custom-made arrayer. Two micrograms of poly(A)$^+$ RNA was labeled with cyanine 5-dUTP or cyanine 3-dUTP. Hybridization and subsequent washes of arrays were performed with a Labeling & Hybridization Kit (MicroDiagnostic). Hybridization signals were measured with a GenePix 4000A scanner (Axon Instruments, Union City, CA) and then processed into primary expression ratios (ratios of cyanine 5-intensity obtained from each sample to cyanine 3-intensity obtained from the rat common reference RNA), which are indicated as 'median of ratios' by the GenePix Pro 3.0 software (Axon Instruments). Normalization was performed for the median of ratios by multiplying normalization factors calculated for each feature on a microarray by the GenePix Pro 3.0 software. The expression ratios were converted into log2 values as final expression ratios.

Animals. All animals were purchased from Japan Crea (Tokyo, Japan) or born and kept under pathogen-free conditions, and cared for in accordance with the guidelines of Keio University School of Medicine.

Rat hernia model. Posterior herniations were created between the 5th and 10th tail IVD of 8-week-old male Wistar rats. After a posterior incision above the IVD was made, the soft tissues such as posterior tendons and ligaments were separated. Then, a small incision was made in AF with subsequent compression between an upper and lower vertebral body to prepare a posterior herniation. Seven days after surgery, rats were sacrificed and the herniated discs with vertebral bodies were removed. For preparation of an IVD section, freshly isolated IVDs were embedded in rat minced liver and frozen using 2-methylbutane (Wako, Osaka, Japan) and liquid nitrogen. Frozen sections of IVD, that had not been decalcified, were obtained using a cryostat (MICROME, model HM505) equipped with a tungsten carbide knife.

Human samples. For the experimental use of the surgical samples, informed consents were obtained from the patients according to the Hospital Ethical Guideline (Keio Hospital #15-52). Specimens of seven chordomas and seven chondrosarcomas diagnosed according to conventional criteria, and three IVD tissues dissected from scoliosis patients as normal IVD were fixed in 4% paraformaldehyde/PBS, embedded in paraffin, and 4 μm sections were cut.

Cell harvest and flow cytometric analysis. NP and AF cells were macroscopically dissected from the cervical, thoracic, and lumber IVD of 8-week-old male Wistar rats. NP tissue was digested with pronase E (0.04%) (SERVA, Heidelberg, Germany) for 1 h at 37 °C and then collagenase P (0.025%) (Roche Diagnosis), for 1 h at 37 °C. To isolate AF cells, AF tissue was treated with pronase E (0.4%) for 1 h at 37 °C, followed by collagenase P (0.025%) for 4 h at 37 °C. Cells were then washed with DMEM/F12 medium (Invitrogen, Carlsbad, CA) containing fetal bovine serum (5%) (Equitech-Bio, Kerrville, TX).

Cells were stained with anti-rat CD24 (clone HIS50, BD PharMingen, San Diego, CA) followed by FITC-conjugated anti-mouse IgG (Biosource, Camarillo, CA). Flow cytometry and cell sorting was performed using FACS Vantage or FACS Calibur (Becton–Dickinson Immunocytometry Systems, San Jose, CA). NP and AF cells were also stained with May-Gruenwald-Giemsa.

Immunohistochemical analysis. Rat IVD were dissected from 8-week-old Wistar rats, fixed in formalin (10%), embedded in paraffin, and cut into 4 μm sections. Deparaffinized sections of paraffin embedded samples or cryosections of rat herniated IVD were stained with anti-rat CD24 (HIS50, BD PharMingen, San Diego, CA, diluted 100-fold) followed by FITC-conjugated anti-mouse IgG (Biosource, Camarillo, CA, diluted 200-fold) and TOTO3 (Invitrogen, diluted 750-fold) for nuclear staining. Antigen retrieval was achieved on chordomas and chondrosarcoma sections by pressure-cooking in citrate buffer (pH 6.0) for 20 min. Samples were then stained with anti-human CD24 (Ab-2, clone 24C02, Neomarkers, Fremont, CA diluted 100-fold) followed by Alexa Fluor488-conjugated anti-mouse IgG (Molecular Probes, Oregon, USA, diluted 100-fold). Immunoreactivity was detected by fluorescence microscopy (Olympus, Tokyo, Japan).

Real-time RT-PCR assay. Total RNA was extracted from NP, AF, pattela tendon, peripheral blood, tibia bone, bone marrow, brain, lens, musculus quadriceps femoris, back skins, spinal cord, white adipose tissue, articular cartilage of femur head, and medial collateral ligaments from the knees of 8-week-old male rats (RNeasy mini kit (Qiagen GmbH, Hilden, Germany) or Trizol (Invitrogen)). First strand cDNA was prepared using the first strand synthesis kit (Invitrogen) according to the manufacturer's instruction, and cDNAs were amplified using a Light Cycler FastStart DNA Master SYBR Green I (Roche diagnostics) in a Light Cycler Quick System (Roche Diagnostics, Mannheim, Germany). Relative mRNA expression levels are shown by comparison with β-actin mRNA expression. The primers used are shown below:

5′-rat β-actin 5′-TCCTAGCACCATGAAGATC-3′,
3′-rat β-actin 5′-AAACGCAGCTCAGTAACAG-3′
5′-rat CD24 5′-TGCTTCTGGCACTGCTCCTAC-3′
3′-rat CD24 5′-GGTGGTAGCATTAGTTGGATTTGG-3′
5′-human β-actin 5′-CGTGACATTAAGGAGAAGC-3′
3′-human β-actin 5′-GGAGTTGAAGGTAGTTTCG-3′
5′-human CD24 5′-GCACTGCTCCTACCCACGCAGATTT-3′
3′-human CD24 5′-GCCTTGGTGGTGGCATTAGTTGGAT-3′

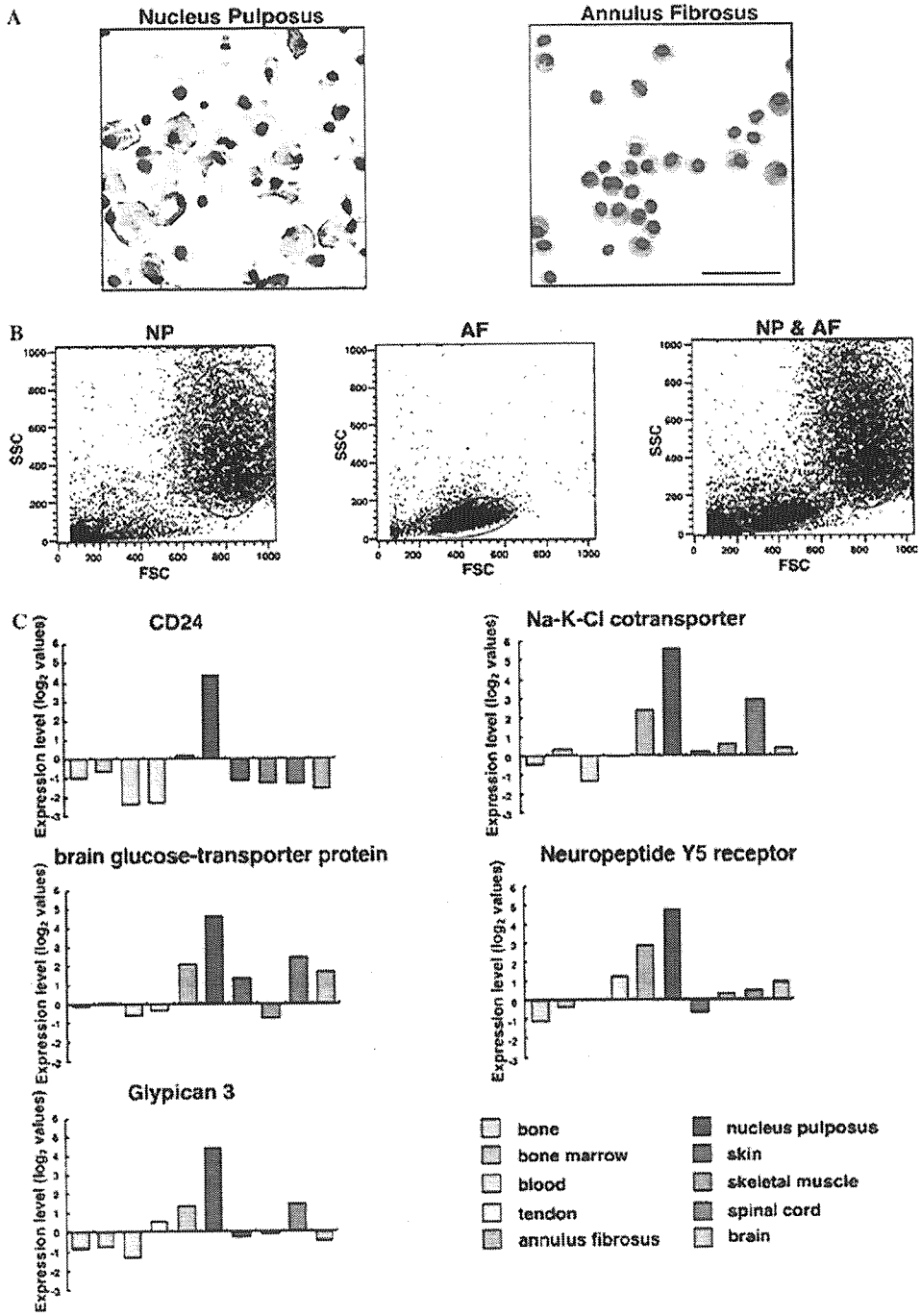

Fig. 1. Identification of NP specific cell surface molecules. Nucleus pulposus (NP) and annulus fibrosus (AF) were isolated from 8-week-old male rat IVD, and their morphology was examined by May-Grunwald-Giemsa staining (A) and flow cytometric analysis (B). Bar = 100 μm. Red and blue circles represent the NP and AF population, respectively. (C) Ten different tissues, including NP and AF, were dissected from 8-week-old male rats, and DNA array hybridization and cluster analysis were performed. Five genes were identified that were expressed highly in NP cells when compared with the other nine tissues.

Results

Identification of NP specific cell factors

To identify cell factors expressed specifically in NP cells, we performed a comparative microarray analysis of 10,490 genes in NP and AF cells, and in cells isolated from tendon, skeletal muscle, spinal cord, brain, skin, bone, bone marrow, and peripheral blood of 8-week-old male Wistar rats. We isolated NP and AF tissues from lumbar, thoracic, and cervical IVD from more than 50 rats, and pooled tissue samples prior to isolation of poly(A)$^+$ RNA. Fig. 1 shows May-Gruenwald-Giemsa staining (Fig. 1A), and flow cyto-

metric analysis (Fig. 1B) of cells isolated from NP and AF tissues. As expected, NP cells had a larger cytoplasm (FSC) and a more complex structure (SSC) when compared to AF cells. We isolated the eight other tissues including tendon, skeletal muscle, spinal cord, brain, skin, bone, bone marrow and peripheral blood from 10 rats, and pooled samples from each tissue. Poly(A)$^+$ RNA was isolated under protease-free conditions to prevent degradation and ensure that we screened a representative pool of poly(A)$^+$ RNA that accurately reflected the levels of expression in cells.

In this report, we focused our efforts on identifying an NP specific cell surface marker that could be utilized to further characterize NP cells. To that end, we chose five cell surface proteins that were specifically expressed at a high level in NP but not in AF cells, or the eight cell types we analyzed (Table 1 and Fig. 1C). These cell factors included: CD24 antigen (NM_012752), Na–K–Cl co-transporter (AF051561), brain glucose-transporter protein (M13979), neuropeptide Y5 receptor (NM_012869), and Glypican 3 (NM_012774). We selected one of the five candidate genes, CD24, for further study since, of the five genes identified, it had the highest level of specific expression in NP cells.

CD24 expression is elevated in NP cells in a tissue specific manner

To determine the relative level of expression of these genes in NP tissue, we used a semi-quantitative real-time PCR assay to determine mRNA expression in NP and AF cells, and the various cell types used in our screen (Fig. 2A). In this experiment we also examined the expression level of CD24 in three additional mesenchymal tissues: white adipose tissue (WAT), articular cartilage, and ligament cells. Our results confirmed that CD24 is specifically expressed in NP cells and that the level of expression was elevated by approximately 4-fold when compared to AF cells. We detected a very low level of CD24 expression in skin and tendon cells, and virtually no expression in the rest of the tissues we examined. We also used a commercially available CD24 antibody to confirm tissue specific expression of CD24 in NP cells using flow cytometry (Fig. 2B), and immunohistochemistry (Fig. 2C). Our results demonstrate that, based on the tissues we examined, CD24 is expressed specifically in NP cells. In addition, CD24 is a useful cell surface marker for identifying NP cells. We have also detected CD24 expression in human NP cells by RT-PCR and immunohistochemical analysis (data not shown).

CD24 is expressed in herniated NP tissue

To further investigate the role of CD24 in IVD disease, we analyzed CD24 expression in a rat model that recapitulates the pathological conditions associated with IVD disease in vivo. Posterior lumbar herniations were created between the 5th and 10th tail IVD. We were able to distinguish herniated protrusions (H) and intact NP (N) (see upper panels Fig. 3). CD24 expression was detected in the herniated protrusion as well as in the remaining NP tissue (lower panels Fig. 3). This result suggests that CD24 may also function in herniated NP tissue.

CD24 is expressed in chordoma cells

Chordoma, a primary malignant tumor of the skeleton, is considered to develop from a remnant of notochordal cells. Chordoma develops mostly in the sacrum region in

Table 1
Microarray identification of highly expressed genes in NP

Accession No.	Tissue									
	Bone	Bone marrow	Blood	Tendon	AF	NP	Skin	Muscle	Spinal cord	Tendon
NM_053518	0.2714	−0.1943	1.4249	0.5499	2.6595	6.3545	−0.2362	−0.6552	0.5039	0.9848
D45920	2.0607	4.421	0	1.6991	1.4552	6.1639	0	0.2857	4.0969	3.1089
AB020019	0.3696	0.2314	1.4082	0.5281	1.8984	5.8966	−0.4461	−0.1219	0.2485	0.585
M13518	0.5917	−0.3147	0.1648	1.542	5.5938	5.8456	−0.1047	−0.484	−0.394	−0.5564
AF051561	−0.454	0.308	−1.3364	−0.0484	2.3934	5.5614	0.2029	0.5763	2.9445	0.3896
NM_031140	1.3829	−0.456	−0.3808	2.6318	1.9309	5.3232	1.0545	−0.255	1.4942	−1.462
XM_217890	0.546	0.9298	0.514	−0.1345	1.301	5.1885	0.5772	0.519	0.4823	0.6012
X62952	1.107	0.5685	−0.8651	2.0374	1.6327	5.0932	0.8891	−0.7298	1.111	−2.0233
AA684960	−0.5951	−0.8135	−0.1959	4.0923	3.3176	4.8973	1.9355	−0.0816	−0.7346	−0.9214
AA686870	−1.9546	−3.2934	−2.7959	4.0689	3.2575	4.886	1.782	−1.2447	−1.7859	−2.0116
AA685376	−0.9828	−1.3808	−0.873	4.1059	2.9635	4.8324	1.9419	−0.0425	−1.152	−1.0262
NM_012869	−1.1392	−0.3696	0.037	1.2284	2.8584	4.7459	−0.6873	0.3208	0.4772	0.9161
AA684929	−0.8034	−0.8288	−0.0499	4.1048	3.2363	4.6141	1.9942	0.0468	−0.9828	−1.0954
M13979	−0.1187	0.0676	−0.606	−0.3364	2.0895	4.5972	1.3437	−0.7984	2.4354	1.6713
NM_012880	2.3417	−4.2379	−4.6439	0.1519	3.4848	4.4875	−3.8783	−4.7959	1.9452	−3.5395
NM_012774	−0.8494	−0.7735	−1.3004	0.514	1.3374	4.4059	−0.2934	−0.1584	1.4626	−0.482
NM_054008	1.9249	0.8237	−0.9296	1.058	0.4823	4.3906	−1.114	−0.7202	0.3161	0.1878
NM_080698	−2.4344	−2.699	−1.1779	4.5453	4.1006	4.3845	−2.9885	0.0014	−2.2042	−1.6943
NM_012752	−0.9799	−0.6804	−2.3884	−2.3004	0.1725	4.3827	−1.1297	−1.2758	−1.3147	−1.5606
AI007530	−0.035	−0.2176	0.704	3.1437	2.5969	4.3677	1.595	−0.2092	−0.3997	−0.3292

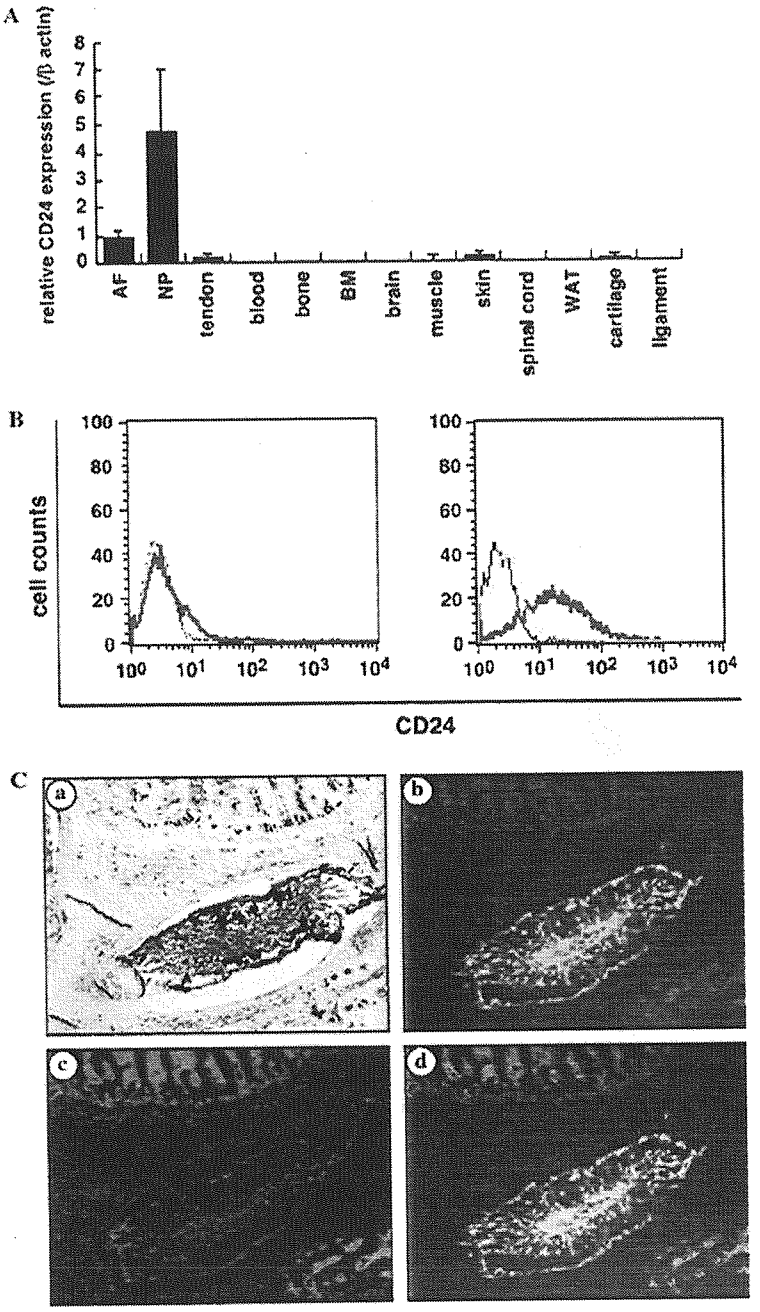

Fig. 2. Confirmation of CD24 expression in NP. (A) CD24 expression was analyzed in 13 different tissues, 10 of which were analyzed in microarray assay, by semi-quantitative real-time PCR. CD24 expression was elevated specifically in NP cells. (B) CD24 expression was analyzed in NP and AF cells using flow cytometry. CD24 expression was detected in NP but not in AF. (C) IVDs were dissected from 8-week-old male rats and stained by rabbit anti-rat CD24 antibody followed by FITC-conjugated anti-rabbit IgG. TOTO3 was used as a counter stain for nuclei. Sections were then stained and examined using phase contrast microscopy (a) and fluorescence microscopy (b–d). (b) CD24, (c) TOTO3, and (d) merged image of CD24 and TOTO3. AF, annulus fibrosis; NP, nucleus pulposus; BM, bone marrow; WAT, white adipose tissue.

elderly patients and local recurrences are frequently observed. Although chordoma cells are considered to derive from the notochord, a comparative evaluation of a tissue specific marker has not been possible. Our identification of CD24 as an NP specific cell marker allowed us to evaluate and compare CD24 expression in notochord, chordoma, and chondrosarcoma, malignant tumors that are derived from mesenchymal cells. Specimens of chordoma and chondrosarcoma were analyzed for CD24 expression (Fig. 4). CD24 expression was detected in six out of the seven chordomas, but not in the seven different chondrosarcomas we analyzed. This result suggests that chordo-

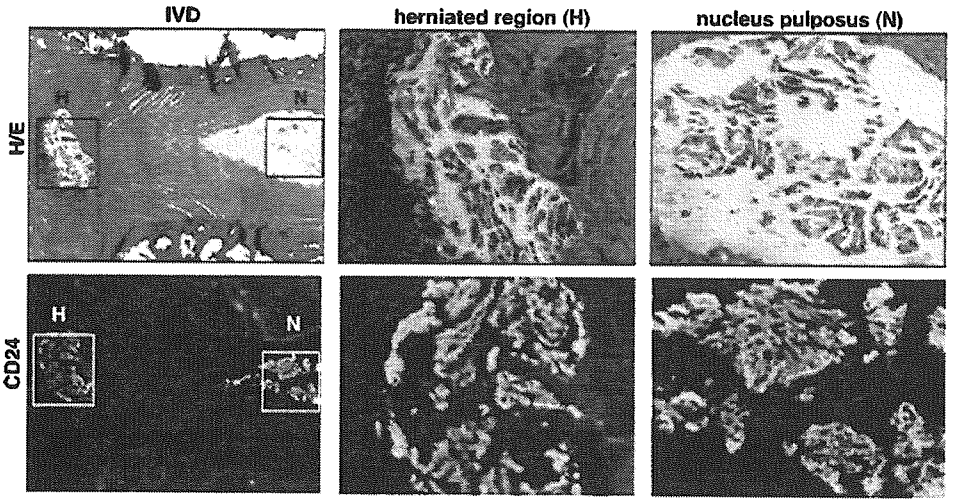

Fig. 3. CD24 expression is detected in herniated protrusion. IVD hernia model was created in 8-week-old rat tail IVDs. Seven days later, IVDs were dissected and stained by H/E (upper panel) or anti-CD24 antibody followed by FITC-conjugated anti-mouse IgG (lower panel), and observed under a fluorescence microscope.

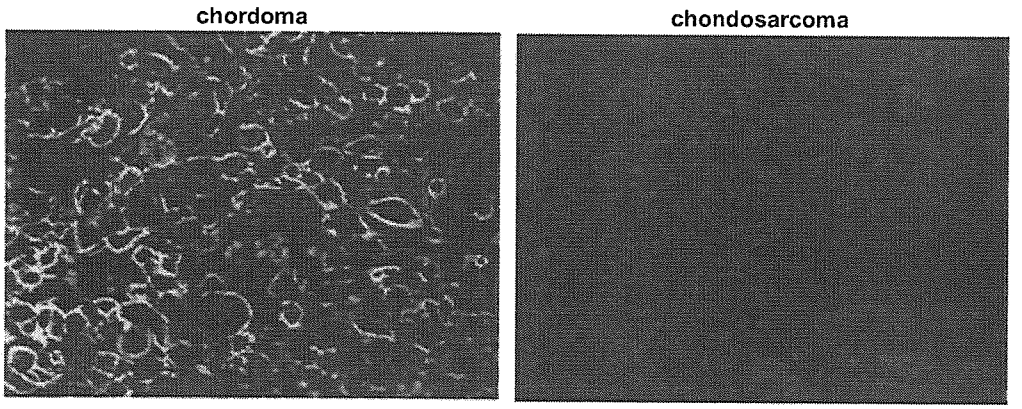

Fig. 4. CD24 expression is detected in chordoma but not in chondrosarcoma. Specimens of chordomas (left panel) and chondrosarcomas (right panel) were stained by anti-human CD24 followed by Alexa Fluor488-conjugated anti-mouse IgG. Immunoreactivity was detected by fluorescence microscopy.

mas are derived from notochordal cells in NP tissue, and that chordoma cells can be distinguished from chondrosarcoma cells by analysis of CD24 expression.

Discussion

We found that expression of CD24 is high in NP cells in a tissue specific manner. To further characterize the function of CD24 in NP tissue, we determined that CD24 is expressed in herniated NP tissue. We also determined that CD24 expression is elevated in chordoma, one of the most common malignant primary neoplasms of the skeleton, which are thought to be a remnant of notochordal cells. The similar pattern of gene expression observed between chordoma and NP supports the hypothesis that chordoma originates from notochordal cells. Interestingly, three out of the five membrane associated factors we identified in this study including: CD24, brain glucose-transporter protein, and the Na–K–Cl co-transporter are also expressed in chordoma (data not shown). Since both NP and chordoma tissues express chondrogenic extracellular matrix protein and aggrecan at high levels, they cannot be used to distinguish chordoma from other chondrogenic malignant tumors [13]. We did not detect CD24 expression in chondrosarcomas, which are malignant tumors derived from mesenchymal cells.

IVD, especially NP is rich in large chondroitin sulfate proteoglycans, which have the ability to retain water in tissues. A large proteoglycan, aggrecan, forms huge aggregates by binding to hyaluronate and links proteins to maintain tissue homeostasis. In contrast, collagens, such as collagen type 2 form a fibrous structure in cartilage. Previous reports indicate that aggrecan and collagen type 9 are involved in IVD maintenance, and more recently, signaling through TGFβ-1 was shown to be important for the expression of both collagen type 2 and aggrecan [1–3]. It

appears that loss of TGFβ-1 signaling in asporin or cartilage intermediate layer protein mutants reduces collagen type 2 and aggrecan expression, and leads to development of osteoarthritis and LDD, respectively [14].

The IVD is an avascular tissue like articular cartilage, tendon, and lens. It remains to be clarified how these avascular tissues are maintained in the absence of oxygenation. One potential explanation is that the fluid surrounding functions in maintaining these tissues under hypoxic conditions. Like NP tissue, the lens is an avascular tissue, and as seen with IVD, degeneration of lens tissue correlates with age. Interestingly, CD24 is also highly expressed in lens (data not shown), indicating CD24 may function to maintain such avascular tissues.

Identification of CD24 as an NP specific marker provides a valuable tool for future studies to ascertain the function of CD24 in the maintenance of NP homeostasis and development of chordomas.

Acknowledgments

We thank the affected individuals for participating in this study: M. Mukai for preparation of specimens of chordoma and chondrosarcoma; Y. Sato and A. Kumakubo for technical support; E.S. Withers-Ward for manuscript preparation.

References

[1] H. Watanabe, K. Nakata, K. Kimata, I. Nakanishi, Y. Yamada, Dwarfism and age-associated spinal degeneration of heterozygote cmd mice defective in aggrecan, Proc. Natl. Acad. Sci. USA 94 (1997) 6943–6947.

[2] S. Annunen, P. Paassilta, J. Lohiniva, M. Perala, T. Pihlajamaa, J. Karppinen, O. Tervonen, H. Kroger, S. Lahde, H. Vanharanta, L. Ryhanen, H.H. Goring, J. Ott, D.J. Prockop, L. Ala-Kokko, An allele of COL9A2 associated with intervertebral disc disease, Science 285 (1999) 409–412.

[3] S. Seki, Y. Kawaguchi, K. Chiba, Y. Mikami, H. Kizawa, T. Oya, F. Mio, M. Mori, Y. Miyamoto, I. Masuda, T. Tsunoda, M. Kamata, T. Kubo, Y. Toyama, T. Kimura, Y. Nakamura, S. Ikegawa, A functional SNP in CILP, encoding cartilage intermediate layer protein, is associated with susceptibility to lumbar disc disease, Nat. Genet. 37 (2005) 607–612.

[4] R.V. Iozzo, A.D. Murdoch, Proteoglycans of the extra cellular environment: clues from the gene and protein side offer novel perspectives in molecular diversity and function, FASEB J. 10 (1996) 598–614.

[5] R.V. Iozzo, The biology of the small leucine-rich proteoglycans. Functional network of interactive proteins, J. Biol. Chem. 274 (1999) 18843–18846.

[6] F. Rannou, T.S. Lee, R.H. Zhou, J. Chin, J.C. Lotz, M.A. Mayoux-Benhamou, J.P. Barbet, A. Chevrot, J.Y. Shyy, Intervertebral disc degeneration: the role of the mitochondrial pathway in annulus fibrosis cell apoptosis induced by overload, Am. J. Patrol. 164 (2004) 915–924.

[7] J. Bruce, F.W. Symington, T.J. McKearn, J. Sprent, A monoclonal antibody discriminating between subsets of T and B cells, J. Immunol. 127 (1981) 2496–2501.

[8] F.W. Symington, S. Hakomori, Hematopoietic subpopulations express cross-reactive, lineage-specific molecules detected by monoclonal antibody, Mol. Immunol. 21 (1984) 507–514.

[9] D.M. Allman, S.E. Ferguson, M.P. Cancro, Peripheral B cell maturation. I. Immature peripheral B cells in adults are heat-stable antigenhi and exhibit unique signaling characteristics, J. Immunol. 149 (1992) 2533–2540.

[10] G. Kristiansen, M. Sammar, P. Altevogt, Tumour biological aspects of CD24, a mucin-like adhesion molecule, J. Mol. Histol. 35 (2004) 255–262.

[11] P.J. Nielsen, B. Lorenz, A.M. Muller, R.H. Wenger, F. Brombacher, M. Simon, T. von der Weid, W.J. Langhorne, H. Mossmann, G. Kohler, Altered erythrocytes and a leaky block in B-cell development in CD24/HSA-deficient mice, Blood 89 (1997) 1058–1067.

[12] O. Li, P. Zheng, Y. Liu, CD24 expression on T cells is required for optimal T cell proliferation in lymphopenic host, J. Exp. Med. 200 (2004) 1083–1089.

[13] D. Gottschalk, M. Fehn, S. Patt, W. Saeger, T. Kirchner, T. Aigner, Matrix gene expression analysis and cellular phenotyping in chordoma reveals focal differentiation pattern of neoplastic cells mimicking nucleus pulposus development, Am. J. Pathol. 158 (2001) 1571–1578.

[14] H. Kizawa, I. Kou, A. Iida, A. Sudo, Y. Miyamoto, A. Fukuda, A. Mabuchi, A. Kotani, A. Kawakami, S. Yamamoto, A. Uchida, K. Nakamura, K. Notoya, Y. Nakamura, S. Ikegawa, An aspartic acid repeat polymorphism in asporin inhibits chondrogenesis and increases susceptibility to osteoarthritis, Nat. Genet. 37 (2005) 138–144.

Available online at www.sciencedirect.com

SCIENCE DIRECT®

Gene 356 (2005) 39 – 48

GENE
SECTION
FUNCTIONAL GENOMICS

www.elsevier.com/locate/gene

Influence of inhalation anesthesia assessed by comprehensive gene expression profiling☆

Atsuhiro Sakamoto[a,*], Jun-ichi Imai[b,c], Akira Nishikawa[c,d], Reiko Honma[b], Emi Ito[b], Yuka Yanagisawa[b], Mika Kawamura[c], Ryo Ogawa[a], Shinya Watanabe[b,*]

[a]*Department of Anesthesiology, Nippon Medical School, Sendagi, Bunkyo-ku, Tokyo 113-8603, Japan*
[b]*Department of Clinical Informatics, Tokyo Medical and Dental University, Yushima, Bunkyo-ku, Tokyo 113-8519, Japan*
[c]*Medicrome, Inc., Sendagaya, Shibuya-ku, Tokyo 151-0051, Japan*
[d]*Nippon Gene, Co., Ltd, Kandanishiki-cho, Chiyoda-ku, Tokyo 101-0054, Japan*

Received 15 October 2004; received in revised form 14 February 2005; accepted 1 March 2005
Available online 20 June 2005
Received by T. Gojobori

Abstract

Although general anesthesia is routinely used as an essential surgical procedure and its harmlessness has been evaluated and endorsed by clinical outcomes, little is known about its comprehensive influence that is not reflected in mortality and morbidity. In this paper, we have shown that inhalation anesthesia affected the expression of < 1.5% of > 10,000 genes, by analyzing the expression profiles for multiple organs of rats anesthetized with sevoflurane. The small number of transcripts affected by the inhalation anesthesia comprised those specific to single and common in multiple organs. The former included genes mainly associated with drug metabolism in the liver and influenced by agents such as amphetamine in the brain. The latter contained multiple circadian genes. In the brain, we failed to detect the alteration of the clock gene expression with the exception of *Per2*, assuming that anesthesia perturbs circadian rhythms. Our findings provide the first assessment for the influence of inhalation anesthesia by approaches of experimental biology and genome science.

Keywords: General anesthesia; Gene expression profile; DNA microarray; Circadian gene; Endothelin1; *Per2*

1. Introduction

Inhalation anesthetics induce general anesthesia that results in unconsciousness, insensitivity to pain, and lack of memory of pain. Although general anesthesia has been routinely used as an essential surgical procedure for approximately 150 years and its harmlessness has been evaluated and endorsed by clinical outcomes (Forrest et al., 1990; Levy, 1984; Brown and Frink, 1993), little is known with regard to its comprehensive influence, which is not reflected in mortality and morbidity. A few studies were reported on the results of inhalation anesthesia on cells and tissues at the molecular level. This anesthetic acted upon an extremely restricted number of genes including those that control the expression of ligand-gated ion channels and G-protein-coupled receptors (Franks and Lieb, 1994; Harris et al., 1995).

The recent progress in genomics enables us to comprehensively describe and analyze the alteration in cells and tissues at the gene expression level by hybridization with DNA microarrays representing genome-wide or subgenome-wide species of transcripts. Therefore, we attempted to comprehensively analyze the effects of

Abbreviations: Arc, activity-regulated cytoskeleton; Bmal1, Brain-Muscle-Arnt-Like-protein 1; Cry2, Cryptochrome2; Dbp, albumin site d-binding protein; Egr1, early growth response gene-1; NGFI-B, nerve growth factor-induced gene B; PCR, polymerase chain reaction; Per2, Period2; SD, standard deviation; Tef, thyrotroph embryonic factor.

☆ Data from all the arrays used in this paper will be available at DDBJ via CIBEX (http://www.cibex.nig.ac.jp/cibex/HTML/index.html) under accession nos.: for the array design, CBX4; for the experiments, CAR4.

* Corresponding authors. Tel.: +81 3 5414 6010; fax: +81 3 5775 1352.
E-mail addresses: no1-saka@nms.ac.jp (A. Sakamoto)
swata@mvc.biglobe.ne.jp (S. Watanabe).

0378-1119/$ - see front matter © 2005 Elsevier B.V. All rights reserved.
doi:10.1016/j.gene.2005.03.022

inhalation anesthesia at the molecular level by obtaining gene expression profiles from rats under inhalation anesthesia.

In this study, we have shown that inhalation anesthesia affected expression of an extremely limited number of genes. This was done by analyzing expression profiles for multiple organs of rats at different time points after anesthetizing with sevoflurane. Our findings could provide a basis for exploring comprehensive influence of inhalation anesthesia and to endorse the safety of anesthesia in the future. The expression profiling analyses also demonstrate the possible association between the anesthetic status and alteration in modulation of the circadian gene expression that were previously identified in addition to nominating novel candidates for the circadian gene.

2. Materials and methods

2.1. Animals and tissue collection

Six-week-old male rats (Wister; Charles River Japan, Inc., Atsugi, Japan) were purchased and adapted to a 12-h light/12-h dark cycle starting at 06:00 and 18:00 for a week before the experiments. The anesthesia experiment was replicated twice with an interval of several weeks between the two experiments (Exp. 1 and Exp. 2). Anesthesia was used at 09:00 on nine rats in Exp. 1 and on 10 rats in Exp. 2. Rats were housed in a plastic box supplied with sevoflurane (4.5% air mixture gas) at the rate of 6 L/min. As the 0-h control, rats ($n=3$, in Exp. 1; $n=4$, in Exp. 2) were subjected to tracheal intubation immediately after induction of anesthesia in order to maintain the anesthetic status and sacrificed to obtain organs. The organs were obtained in the order of the blood, the spleen, the kidneys, the liver, the lungs, the heart, and the brain within 5–10 min per animal after the intubation. As the 2-h and 6-h samples, the anesthetized rats were picked up from the plastic box supplied with sevoflurane, subjected to the intubation, and sacrificed to similarly obtain the organs 2 h and 6 h after induction of anesthesia, respectively. Three rats were used for each time point of each experiment with the exception of the time point of 0 h in Exp. 2, in which four rats were used; eventually, a total of 19 rats were used in the two replicated experiments.

2.2. RNA preparation

The blood obtained was immediately mixed with an ISOGEN-LS reagent (NIPPON GENE, Tokyo, Japan) after dilution with an equal volume of water. The other organs (the whole brain, the whole heart, the left lung, the lateral left lobe of the liver, the whole spleen, and both the kidneys) were immediately frozen in liquid nitrogen and lysed with an ISOGEN reagent (NIPPON GENE). Total RNA was prepared from the lysate in accordance with the manufacturer's instructions. Poly(A)+ RNA was prepared from total RNA with a Poly(A) Purist Kit (Ambion, TX, USA), in accordance with the manufacturer's instructions.

2.3. Microarray preparation and expression profile acquisition

A set of synthetic polynucleotides (80-mers) that represented 11,464 rat transcripts derived from 10,490 independent genes, including most of the RefSeq clones deposited in the NCBI database (MicroDiagnostic, Tokyo, Japan), was arrayed on a slide glass (S9115; Matsunami, Kishiwada, Japan) with a custom-made arrayer (Kobayashi et al., 2004; Ito et al., 2003). Poly(A)+ RNA (2 μg) was labeled with SuperScript II (Invitrogen, CA, USA) and Cyanine 5-dUTP for each sample or Cyanine 3-dUTP (PerkinElmer, MA, USA) for a rat common reference RNA (MicroDiagnostic). Labeling, hybridization, and subsequent washes of microarrays were performed with a Labeling and Hybridization Kit (MicroDiagnostic), in accordance with the manufacturer's instructions. The rat common reference RNA was purchased as a single batch and labeled as an aliquot with Cyanine-3 for a single microarray side by side with each sample which was labeled with Cyanine-5. Hybridization signals were measured using a GenePix 400A scanner (Axon Instruments, CA, USA) and then processed into primary expression ratios ([Cyanine 5-intensity obtained from each sample]/[Cyanine 3-intensity obtained from the rat common reference RNA], which are indicated as 'median of ratios' in GenePix Pro 3.0 software (Axon Instruments)). Normalization was performed for the median of ratios (primary expression ratios) by multiplying normalization factors calculated for each feature on a microarray by the GenePix Pro 3.0 software. All the data in accordance with the MIAME guideline were deposited at DDBJ via CIBEX (http://www.cibex.nig.ac.jp/cibex/HTML/index.html) under accession numbers CBX4 (for the array design) and CAR4 (for the experiments).

2.4. Data analysis

Data processing and subsequent hierarchical clustering analysis were performed with an Excel program (Microsoft, WA, USA) and an MDI gene expression analysis software package (MicroDiagnostic). The primary expression ratios were converted into $\log_2$ values ($\log_2$ Cyanine-5 intensity/Cyanine-3 intensity) (designated log ratios) and compiled into a matrix (designated primary data matrix).

We conducted the following operations to extract genes, from the primary data matrix, in which the expression levels altered specifically on inhalation anesthesia. (i) The mean average of log ratios for each 0-h data set of each organ (designated 0-h averages) was calculated. (ii) The relative ratios against the respective 0-h average values for all the log ratios (designated relative log ratios) were generated. This enabled us to compare all data as expression differences that deviated from the mean average

of each gene and to introduce a single threshold value (=0.75) to filter the genes in which the expression levels altered. (iii) All the relative log ratios were arranged into a matrix (designated secondary data matrix). (iv) In order to filter out the genes in which the expression levels deviated from the mean average in an individual data set for each gene, each time point, and each organ, we calculated standard deviation of relative log ratios for each time point and each organ, using the data from all the animals (Exp. 1 and Exp. 2). The SD values calculated by every organ showed similar distributions and there was no obvious correlation between the SD values and the fluorescent intensities initially detected in each microarray. This enabled us to introduce a single SD value (=1.0) as a cutoff threshold for all the genes. The calculated value should reflect the differences between independently repeated anesthetic experiments and the responses of individual rats. (v) The genes with standard deviation of the relative log ratios greater than 1 for at least one time point for each organ were detected from the secondary data matrix. (vi) The genes with relative log ratios commonly greater than 0.75 or uniformly smaller than −0.75 in each organ among at least five individual rats, which had an identical anesthetic period (2 h or 6 h), were selected from the secondary data matrix.

Next, we extracted genes, in which expression patterns were specific to a single organ or common to multiple organs from the secondary data matrix by the following operations. (i) The mean average of log ratios for 2 h or 6 h for each organ (designated 2-h and 6-h averages) was calculated. (ii) The relative ratios of 2-h and 6-h averages against 0-h average for each organ (designated relative 2-h and 6-h averages) were generated. (iii) Genes with relative 2-h average or relative 6-h average greater than 0.75 or lower than −0.75 in a single organ were selected. (iv) Genes with relative 2-h average or relative 6-h average greater than 0.75 or lower than −0.75 in any two organs were selected. (v) Genes with relative 2-h average or relative 6-h average was greater than 0.75 or lower than −0.75 in any three organs were selected. (vi) Genes with relative 2-h average or relative 6-h average greater than 0.75 or lower than −0.75 in any four organs were selected. (vii) Genes with relative 2-h average or relative 6-h average greater than 0.75 or lower than −0.75 in more than four organs were selected.

3. Results

In order to comprehensively evaluate the influences of general anesthesia at the gene expression level, we obtained seven major organs from rats under general anesthesia with sevoflurane, an inhalation anesthetic, at 0 h, 2 h, and 6 h after induction of anesthesia. We performed the animal experiment with sevoflurane twice with an interval of several weeks between the two experiments (designated as Exp. 1 and Exp. 2). In Exp. 1, we used three rats for each time point and obtained for the seven organs but failed to draw peripheral blood from a rat assigned for 2 h. In Exp. 2, we used four rats for 0 h and three rats for 2 h and 6 h, respectively, and failed tissue lysate preparation from the lungs and liver of a rat assigned for 0 h. Eventually, we obtained 130 independent tissue samples for the three time points. We labeled poly(A)+ RNA purified from the samples and a rat common reference RNA with Cyanine-5 and Cyanine-3, respectively, and hybridized to microarrays representing 11,464 transcripts derived from 10,490 individual genes. Hybridization signals were processed into expression ratios as $\log_2$ values (designated log ratios) and compiled into a matrix designated as the primary data matrix (see Materials and methods). Data from all the arrays used in this paper are available at DDBJ via CIBEX (http://www.cibex.nig.ac.jp/cibex/HTML/index.html) under accession numbers CBX4 (for the array design) and CAR4 (for the experiments).

3.1. Overview of gene expression patterns in rat tissues after being subjected to general anesthesia

First, we sought to seize an overview of the experiments conducted in this study by two-dimensional clustering analysis of log ratios calculated from primary expression ratios against the common reference RNA (primary data matrix), prior to extracting genes that were affected by inhalation anesthesia at the expression level. The primary data matrix should enable us to relatively compare all samples one another without conducting direct comparison by hybridization on an identical microarray. We predicted that the most obvious differences obtained from the clustering analysis of the primary data matrix should be those reflecting tissues examined in this study, represented as sample clusters consisting of each organ only (tissue clusters) in a single dendrogram. Furthermore, we presumed that we might be able to compare gene expression levels that were associated with different experimental conditions within each tissue cluster in the dendrogram.

We extracted genes with log ratios over 1 or under −1 in at least one sample from the primary data matrix and subjected them to two-dimensional hierarchical clustering analysis for samples and genes (Fig. 1) (Schena et al., 1996; Lyons et al., 2000). When the clustering analysis for the samples was performed, the greatest seven clusters corresponding to the individual organs were obtained as predicted. The clusters representing the lungs, heart, liver, and blood comprised two smaller clusters completely corresponding to differences between Exp. 1 and Exp. 2, reflecting experimental errors. The clusters representing the kidney and brain consisted of two smaller clusters that incompletely corresponded to the experiment differences with some exceptions. With the exception of the smaller cluster in Exp. 1, representing the liver, in which three

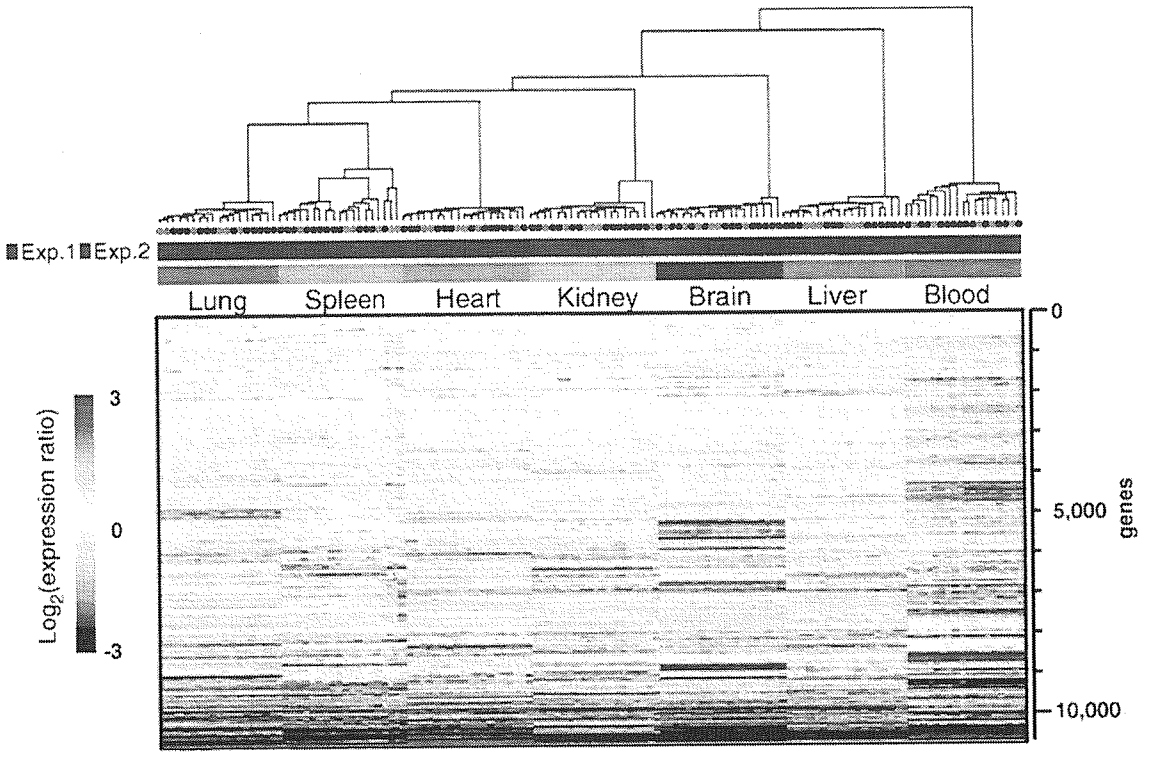

Fig. 1. Gene expression profiles obtained from seven organs of rats under inhalation anesthesia. Rows and columns represent genes (10,796) and samples (130), respectively. The genes and samples are assembled in the order obtained from the results of the two-dimensional hierarchical clustering analysis. Dendrogram at the top of the figure indicates the relationship among the samples after clustering analysis; the y-axis of the dendrogram depicts Euclid square distance as the dissimilarity coefficient. The color bar on the left side of the figure shows expression ratio against the common reference RNA in $\log_2$; red and blue indicate increase and decrease of the expression ratios, respectively. Solid circles indicate individual rats assigned for 0 h, 2 h, and 6 h by black, green, and red, respectively. Red and blue bars show two independent anesthesia experiments, i.e., Exp. 1 and Exp. 2, respectively. Color bars in pink, light blue, orange, violet, dark blue, light green, and gray represent the lungs, spleen, heart, kidney, brain, liver, and blood, respectively.

different time points formed the three smallest clusters, the smaller clusters by the differences in experiment were not divided by differences of anesthetic periods but by the individual differences among rats. These results obtained from the clustering analysis for the 130 samples indicate that differences among anesthesia periods with regard to the expression profiles of over 10,000 genes are much smaller than differences among individual rats, independent experiments, and organs.

3.2. Selection of genes in which expression patterns were affected by inhalation anesthesia

In order to extract genes in which expression levels altered specifically due to inhalation anesthesia, from the primary data matrix, we conducted the operations described in the Materials and methods and generated the secondary data matrix comprising relative log ratios. From the secondary data matrix, we successfully obtained 177 transcripts originating from 167 genes that satisfied the conditions described in the Materials and methods and subsequently subjected the data of the 177 transcripts to clustering analysis for genes (Fig. 2). Clustering analysis demonstrated that the 167 genes comprised those genes specific to a single organ and common in different organs. It also demonstrated that among the organs tested in this study, expression alteration of 114 genes was predominantly detected in the liver and that of 42 genes was predominantly detected in the lungs and the expression alteration of a few genes was predominantly detected in the blood, brain, heart, kidney, and spleen. Moreover, we noticed that the alteration of expression levels was detected mainly in the longer period but rarely in the shorter period. These results confirm that the inhalation anesthesia affected expression of a small number of genes except for the liver. This result was also confirmed by the two-dimensional clustering analysis for the primary data matrix of over 10,000 genes.

3.3. Expression profiles for genes that are immediately affected by anesthesia

Next, we extracted genes whose expression levels were immediately affected by the inhalation anesthesia, particularly in the shorter period by filtering operations similar to those described above. The reason was the following. Although we noticed that the predominant alteration appeared at the time point of 6 h, we expected the possibility that the data obtained at 2 h might provide information on genes that may specifically regulate the expression of the

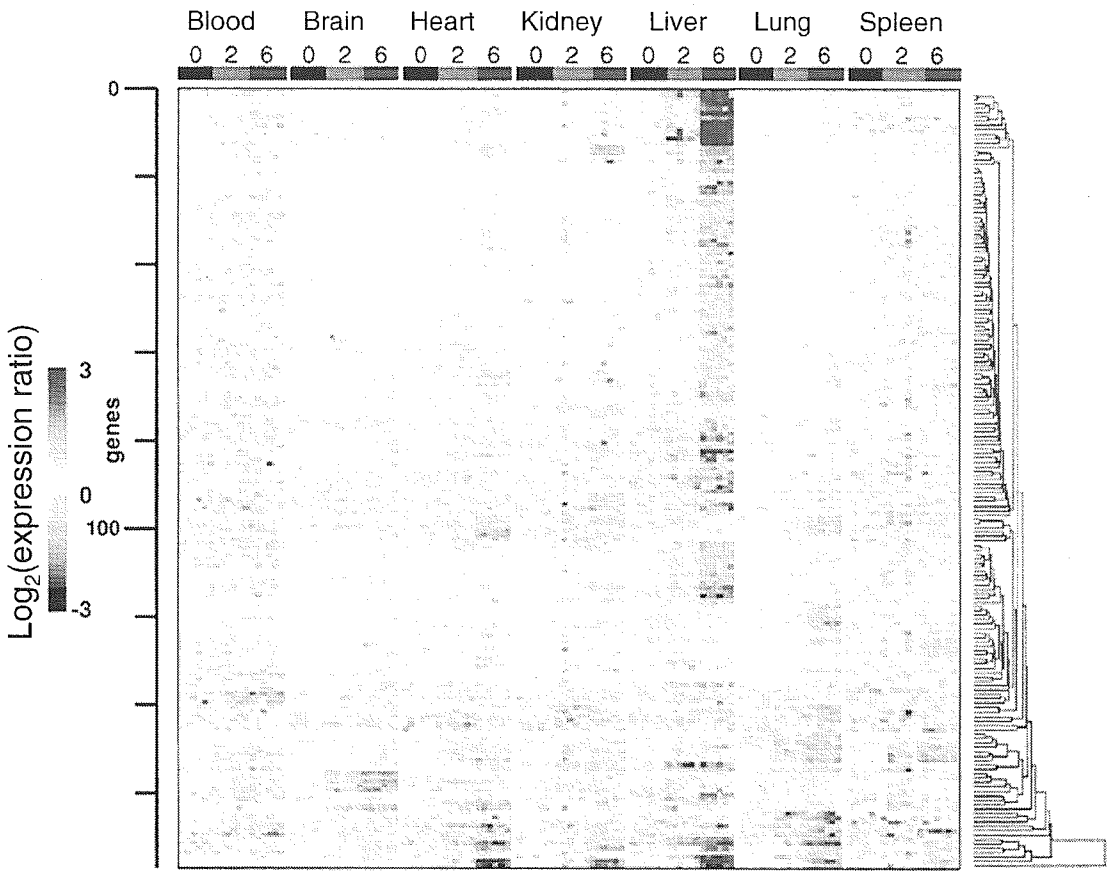

Fig. 2. Clustering analysis of genes in which expression levels were obviously altered in an inhalation anesthesia-specific manner. Rows and columns represent genes and samples, respectively. Rows are assembled in the order derived from clustering analysis. Columns are assembled in the order of organs and time points; black, green, and red bars exhibit 0-h, 2-h, and 6-h samples, respectively. Dendrogram on the right side of the figure indicates the relationship of genes after clustering. The color bar on the left side of the figure shows expression ratio against the common reference RNA in $\log_2$; red and blue indicate increase and decrease of the expression ratios, respectively. Color bars in pink, light blue, orange, violet, dark blue, light green, and gray represent the lungs, spleen, heart, kidney, brain, liver, and blood, respectively.

genes affected in the later phase. We obtained only 20 transcripts derived from 18 genes, as genes affected immediately by the inhalation anesthesia (Fig. 3). These results indicate that in the early phase, an extremely small number of genes are affected by inhalation anesthesia (approximately 0.17% of the total genes tested). Among the 20 transcripts, 18 exhibited single organ-specific expression patterns but only two represented those common in multiple organs. One of the two genes common to the multiple organs was a gene previously known as the circadian gene, *Rev-ErbA-alpha* (Leloup and Goldbeter, 2003). We notice that the gene expressing vasoconstrictor endothelin 1 (Yanagisawa et al., 1988) was upregulated as an early responsive gene in the lungs. This may be because inhalation anesthetics are initially exposed at the highest concentration to the lungs as compared to the otherorgans.

3.4. Extraction of genes in which expression was influenced by inhalation anesthesia in an organ-specific manner

We extracted genes in which expression patterns were specific to a single organ or common in different organs by the operations described in the Materials and methods. Subsequently, we selected genes that satisfied the conditions described in the Materials and methods from the genes shown in Fig. 2. We classified the selected genes in which the expression patterns were influenced by the inhalation anesthesia, as shown in Fig. 4a–e.

In the liver, we detected the maximum number of genes in which the expression was influenced by the inhalation anesthesia (99 transcripts; approximately 56% of the total genes influenced). These liver-specific genes include those characterized as the drug metabolism-associated or the drug response-associated genes such as cytochrome *P*450s (Lu, 1998), epoxide hydrolases (Cannady et al., 2002), UDP-glucuronosyl transferases (Mackenzie et al., 1997), and glutathione sulfotransferases (Snyder and Maddison, 1997). We obtained the second highest number of influenced genes in the lungs (15 transcripts). Since anesthetics act on the brain and induce unconsciousness, we focused on the genes in which the expression specifically influenced the brain. We did not observe an elevation of expression levels of any genes in the brain but detected four genes in which expression levels decreased after the induction of the inhalation

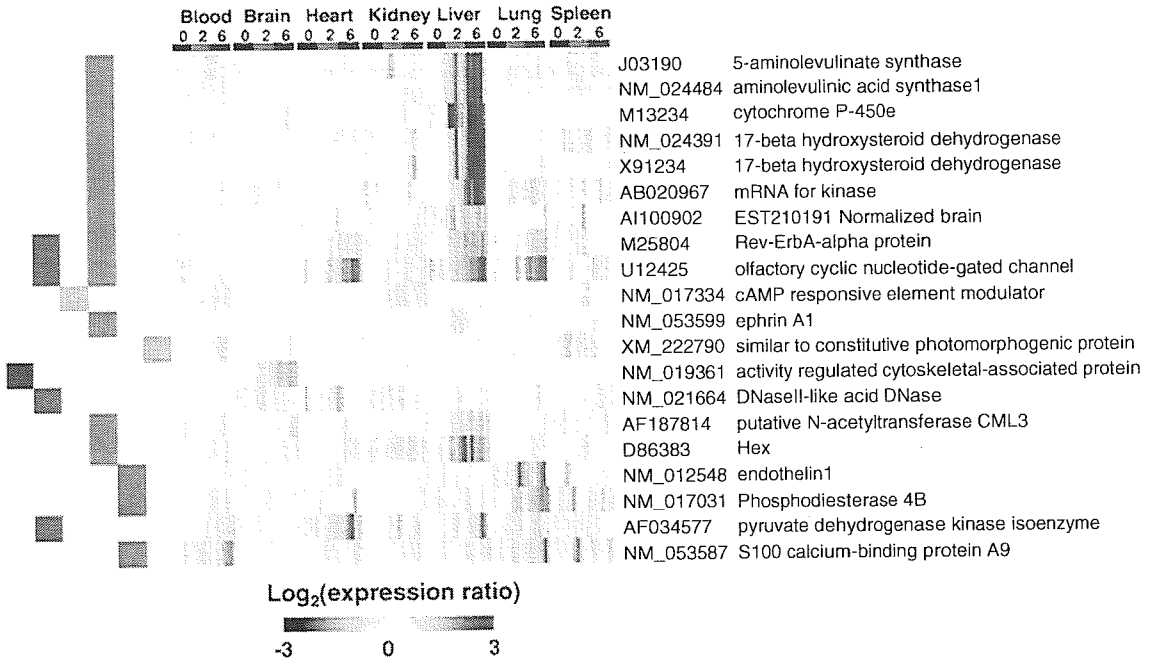

Fig. 3. Genes in which expression levels altered in the early phase (2 h) of inhalation anesthesia. The genes are assembled in the order obtained from the results of hierarchical clustering analysis. The color bar at the bottom of the figure shows expression ratio against the common reference RNA in $\log_2$; red and blue indicate increase and decrease of the expression ratios, respectively. Color bars in pink, light blue, orange, violet, dark blue, light green, and gray represent the lungs, spleen, heart, kidney, brain, liver, and blood, respectively.

anesthesia (*Arc* (Link et al., 1995), *NGFI-B* (Maruyama et al., 1998), *Krox20* (Bhat et al., 1992), and *Egr1* (Liu et al., 1996)). These four genes were previously reported to encode transcription factors and to be those in which the expression levels were differently affected by treatment with the agents acting on the central nervous system (CNS), such as amphetamine (Gonzalez-Nicolini and McGinty, 2002), cocaine (Freeman et al., 2002), pentobarbital (Ryabinin et al., 2000), and antidepressants (Pei et al., 2003).

3.5. Evaluation of genes in which expression was altered during inhalation anesthesia in a multiple organ-common manner

As described above, we notice that several genes were affected during anesthesia in a similar manner among multiple organs. These included the previously reported circadian genes in which the expression level alters with an oscillating rhythm based on whether it is day or night. We selected expression data for the representative circadian genes from the secondary data matrix (Fig. 5). Most temporal expression patterns for known circadian genes obtained in this study were consistent with those reported previously with the exception of the genes from the brain (Ueda et al., 2002; Storch et al., 2002; Panda et al., 2002). In the brain, we observed no alteration of the expression of the known circadian genes during anesthesia with the exception of *Per2*. The *Per2* gene provided an expression pattern contradictory to those reported previously, representing decreased expression levels during the day. Furthermore, we compared expression patterns obtained in this study with those recently reported for the mouse circadian genes using the microarray technology (Ueda et al., 2002). The rat orthologues of the mouse circadian genes in the brain exhibited no alteration of expression during the inhalation anesthesia. The genes compared will be listed in Supplementary Information Table 6 (http://www.cibex.nig.ac.jp/cibex/HTML/index.html; under accession no. CAR4). These findings indicate that under inhalation anesthesia, the circadian rhythm may differ from normal circadian rhythms.

4. Discussion

By analyzing expression profiles obtained from rats under general anesthesia,we have shown that inhalation anesthesia affected expression of a small number of genes.

Fig. 4. Classification of genes that showed alteration in expression levels during anesthesia by the number of the organs in which the alteration was detected. a, genes in which expression levels altered in a single organ-specific manner. The genes of each gene set for a specific organ are assembled in the order derived from clustering. b, c, d, e, and f, genes in which expression levels altered commonly in two, three, four, and more than four organs, respectively. The color bar at the bottom of the figure shows expression ratio against the common reference RNA in $\log_2$; red and blue indicate increase and decrease of the expression ratios, respectively. Color bars in pink, light blue, orange, violet, dark blue, light green, and gray represent the lungs, spleen, heart, kidney, brain, liver, and blood, respectively.

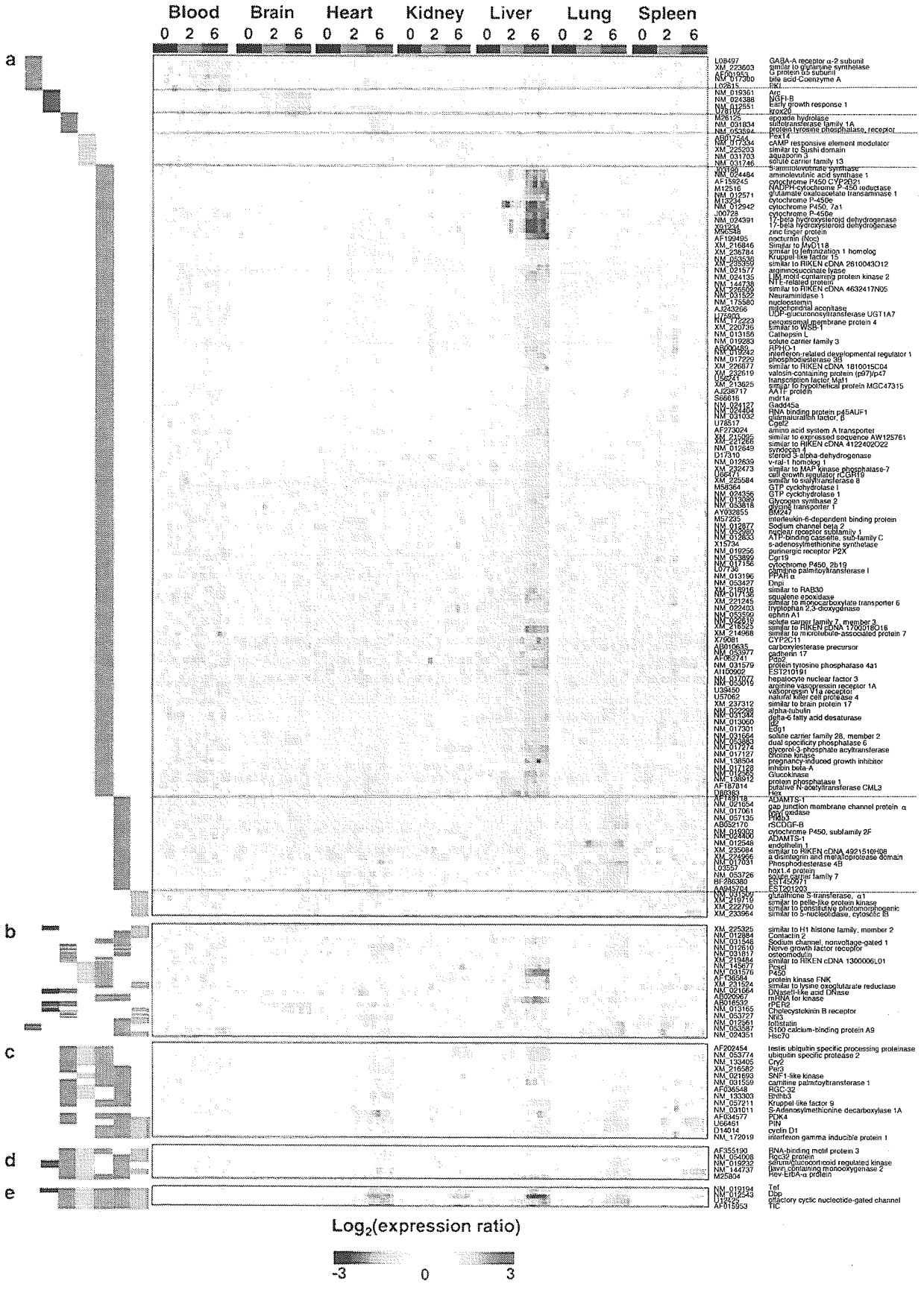
Blood
Brain
Heart
Kidney
Liver
Lung
Spleen
0 2 6
a
b
c
d
e
L08497 GABA-A receptor α-2 subunit
XM_223603 similar to glutamine synthetase
AF551051 G protein αs subunit
NM_017300 bile acid-Coenzyme A
L02815 Rkd
NM_019361 Arc
NM_024388 NGFI-B
NM_012551 early growth response 1
U28106 krox20
M26125 epoxide hydrolase
NM_031834 sulfotransferase family 1A
NM_053594 protein tyrosine phosphatase, receptor
AB072644 Ptex14
NM_017334 cAMP responsive element modulator
XM_225203 similar to Sushi domain
NM_031703 aquaporin 3
NM_031746 solute carrier family 13
M97580 5-aminolevulinate synthase
NM_024484 aminolevulinic acid synthase 1
AF159245 cytochrome P450 CYP26B1
M12516 NADPH-cytochrome P-450 reductase
NM_012571 glutamate oxaloacetate transaminase 1
M19234 cytochrome P-450e
NM_012942 cytochrome P450, 7a1
J00728 cytochrome P-450e
NM_024391 17-beta hydroxysteroid dehydrogenase
X91234 17-beta hydroxysteroid dehydrogenase
M96549 zinc finger protein
AF199495 nocturnin (Noc)
XM_216846 Similar to MyD118
XM_236784 similar to fethrinatrion 1 homolog
NM_053536 Kruppel-like factor 15
XM_235359 similar to RIKEN cDNA 2610043O12
NM_021577 argininosuccinate lyase
NM_024135 LIM-motif-containing protein kinase 2
NM_144738 NT6-related protein
XM_235609 similar to RIKEN cDNA 4632417N05
NM_031522 Neuraminidase 1
NM_175580 nucleostemin
AJ243266 mitochondrial aconitase
U78900 UDP-glucuronosyltransferase UGT1A7
NM_172223 peroxisomal membrane protein 4
XM_220736 similar to WSB-1
NM_013156 Cathepsin L
NM_019283 solute carrier family 3
AB004469 APHO-1
NM_019242 interferon-related developmental regulator 1
NM_017229 phosphodiesterase 3B
XM_226877 similar to RIKEN cDNA 1810015C04
XM_232619 valosin-containing protein (p97)/p47
U56427 transcription factor Maf1
XM_213625 similar to hypothetical protein MGC47315
AJ238717 AATF protein
S66616 nur1a
NM_024127 Gadd45a
NM_024404 RNA binding protein p45AUF1
NM_031032 glutamate/aspartate factor, β
U78517 Cgef2
AF273024 amino acid system A transporter
XM_215695 similar to expressed sequence AW125761
XM_221266 similar to RIKEN cDNA 4122402O22
NM_012649 syndecan 4
D17310 steroid 5-alpha-dehydrogenase
NM_012639 v-ral-1 homolog 1
XM_232473 similar to MAP kinase phosphatase-7
U66477 cell growth regulator rCGR19
XM_225584 similar to sialyltransferase 8
M58364 GTP cyclohydrolase I
NM_024356 GTP cyclohydrolase 1
NM_013099 Glycogen synthase 2
NM_053818 glycine transporter 1
AY032855 BM249
M57295 interleukin-6-dependent binding protein
NM_012877 Sodium channel beta 2
NM_052980 nuclear receptor subfamily 1
NM_012833 ATP-binding cassette, sub-family C
X15794 s-adenosylmethionine synthetase
NM_019256 purinergic receptor P2X
NM_053899 Cgr19
NM_017156 cytochrome P450, 2b19
L07736 carnitine palmitoyltransferase I
NM_013196 PPAR α
NM_053427 Dnpi
XM_216916 similar to RAB30
NM_017136 squalene epoxidase
XM_221245 similar to monocarboxylate transporter 6
NM_022403 tryptophan 2,3-dioxygenase
NM_053559 ezrin/radixin/moesin (ERM) family member
NM_022619 solute carrier family 7, member 3
XM_218525 similar to RIKEN cDNA 1700016G16
XM_214968 similar to microtubule-associated protein 7
X79081 CYP2C11
AB010635 carboxylesterase precursor
NM_053977 cadherin 17
AF182741 Ptp2
NM_031579 protein tyrosine phosphatase 4a1
AI100902 EST1210191
NM_017077 hepatocyte nuclear factor 3
NM_053019 arginine vasopressin receptor 1A
U39450 vasopressin V1a receptor
U57062 natural killer cell protease 4
XM_237312 similar to brain protein 17
NM_022298 alpha-tubulin
NM_031344 delta-6 fatty acid desaturase
NM_013060 Ptp
NM_017301 Cdg1
NM_031664 solute carrier family 28, member 2
NM_053983 dual specificity phosphatase 6
NM_017272 glycerol-3-phosphate acyltransferase
NM_017127 choline kinase
NM_138504 pregnancy-induced growth inhibitor
NM_017128 inhibin beta-A
NM_012565 Glucokinase
NM_138912 protein phosphatase 1
AF187814 putative N-acetyltransferase CML3
D86363 Hex
AF149118 ADAMTS-1
NM_021654 gap junction membrane channel protein α
NM_017061 Ddc/ gadase
NM_057135 Phb3
AB052170 rSCD3F-B
NM_019909 cytochrome P450, subfamily 2F
NM_024406 ADAMTS-1
NM_012548 endothelin 1
XM_235084 similar to RIKEN cDNA 4921510H08
XM_224956 a disintegrin and metalloprotease domain
NM_017031 Phosphodiesterase 4B
U03257 hox1.4 protein
NM_053726 solute carrier family 7
BF286380 EST459971
AA957014 EST301203
NM_017076 glutathione S-transferase, α1
XM_219776 similar to pelle-like protein kinase
XM_222790 similar to constitutive photomorphogenic
XM_233964 similar to 5-nucleotidase, cytosolic IB
XM_225325 similar to H1 histone family, member 2
NM_012884 Contactin 2
NM_031548 Sodium channel, nonvoltage-gated 1
NM_012610 Nerve growth factor receptor
NM_031817 osteomodulin
XM_219464 similar to RIKEN cDNA 1300006L01
NM_145677 Pcsd
NM_031576 P450
AF136564 protein kinase FNK
XM_231524 similar to lysine oxoglutarate reductase
NM_021664 DNaseII-like acid DNase
AB029967 mRNA for kinase
AB016539 rPER2
NM_013165 Cholecystokinin B receptor
NM_053727 Nfil3
NM_012561 follistatin
NM_053587 S100 calcium-binding protein A9
NM_024351 Hsc70
AF202454 testis ubiquitin specific processing proteinase
NM_053774 ubiquitin specific protease 2
NM_133405 Cry2
XM_216582 Per3
NM_021693 SNF1-like kinase
NM_031559 carnitine palmitoyltransferase 1
AF036548 RGC-32
NM_133303 bhlhb3
NM_057211 Kruppel-like factor 9
NM_031011 S-Adenosylmethionine decarboxylase 1A
AF034577 PDK4
U66461 PIN
D14014 cyclin D1
NM_172019 interferon gamma inducible protein 1
AF355190 RNA-binding motif protein 3
NM_054008 Npc32 protein
NM_019232 serum/glucocorticoid regulated kinase
NM_144737 flavin containing monooxygenase 2
M25804 Rev-ErbA-α protein
NM_019194 Tef
NM_012543 Dbp
U12422 olfactory cyclic nucleotide-gated channel
AF015953 TIC
Log2(expression ratio)
-3
0
3

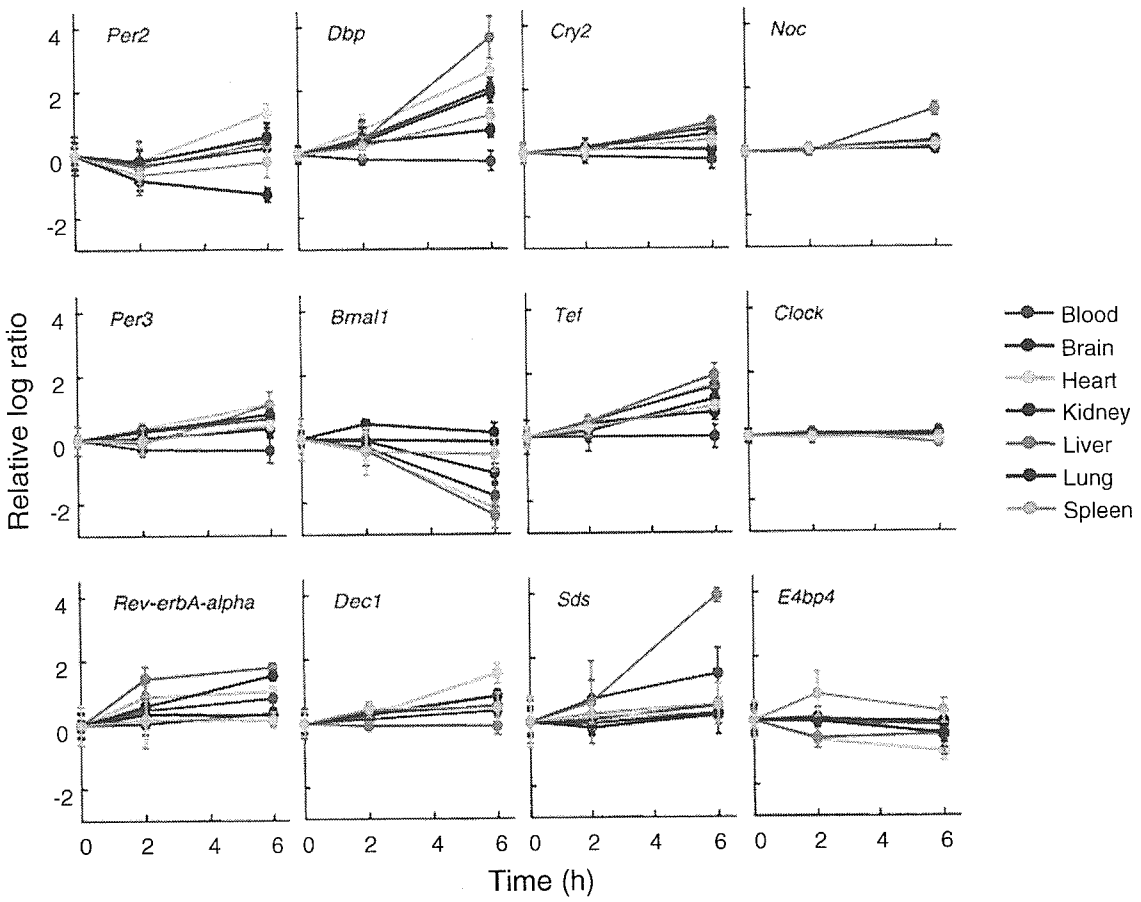

Fig. 5. Expression kinetics of the rat orthologues for the previously identified mouse circadian genes in rats under inhalation anesthesia. Relative log ratios were extracted from the secondary data matrix for the following genes: *Clock*, *Per2*, *Cry2*, *Per3*, *Noc*, *Tef*, *Rev-erbA-alpha*, *Dbp*, and *Bmal1*. The extracted relative log ratios were subjected to calculation of mean average (solid circle) and standard deviation (error bar) for each time point of individual organs. The *x* and *y* axes show time (h) and relative log ratio against the 0-h control, respectively. Graphs in pink, light blue, orange, violet, dark blue, light green, and gray represent the lungs, spleen, heart, kidney, brain, liver, and blood, respectively.

Our study should provide the first comprehensive assessment for the influence of inhalation anesthesia with regard to experimental biology and genome science. Although we did not observe obvious alterations for the majority of genes tested, we successfully detected genes in which expression levels were influenced in an inhalation anesthesia-dependent manner.

Among the genes in which expression levels altered in an anesthesia-dependent manner, the most predominant gene cluster was found in the samples obtained from the liver. The genes will be listed in Supplementary Information Table 4 (http://www.cibex.nig.ac.jp/cibex/HTML/index.html; under accession no. CAR4). These liver-specific genes include many cytochrome *P*450s, UDP-glucuronosyl transferases, and glutathione sulfotransferases, representing involvement and activation of drug-metabolizing enzyme systems by hydroxylation, glucuronide conjugation, and glutathione conjugation, respectively (Lu, 1998; Cannady et al., 2002; Mackenzie et al., 1997; Clarke et al., 1997). This indicates that almost all the genes in the enzyme systems previously identified to be involved in drug metabolism in the liver are engaged (Gerhold et al., 2001). However, it is rather predictable that an inhalation anesthetic induces the expression of the drug metabolism-related genes as a toxicological response. On the other hand, as novel findings, our data propose that many transcripts (thus far uncharacterized) may be regulated by a common set of trasncription factors, in addition to being involved in the metabolism of the anesthetic in a similar manner to the genes for drug-metabolizing enzymes that were previously identified. Moreover, we presume that the induction of endothelin at the early phase of anesthesia in the lungs represents one of the toxicological responses and that endothelin possibly induces some effects in the vascular system, particularly in the early phase of the anesthetic period. This is presumed because the induction of the endothelin gene expression has been previously reported as responses to toxins (Sonin et al., 1999; Baveja et al., 2002). It needs to be investigated whether other anesthetics affect the expression of the genes in a manner similar to sevoflurane, as demonstrated in this study. Such a comparative study would provide information that is necessary to assess the side effects of the currently available anesthetics and to develop safe tools in anesthesiology.

We should mention that the findings presented here may not provide direct evidence to suggest that the anesthetic causes the anesthetic status by inducing alteration in the expression of certain genes since we did not detect many regulated genes in the brain, which should comprise the main target of the anesthetic. Despite the low number of regulated genes (3 up, 6 down), these genes encode transcription factors and circadian rhythm genes that were previously reported to be increased by amphetamine (Gonzalez-Nicolini and McGinty, 2002), cocaine (Freeman et al., 2002), and morphine withdrawal (Ammon et al., 2003), whereas their expression decreases by anesthesia with an intravenous anesthetic (Ryabinin et al., 2000).

One of the interesting findings of this study is that several circadian genes exhibited alteration of expression during an anesthetic period in a multiple organ-common manner. However, in the brain, we obtained several findings that were inconsistent with those reported previously (Ueda et al., 2002). We did not detect an alteration in several genes in which expression exhibited the circadian rhythm and we observed contradictory kinetics in the expression of *Per2*. The hypothesis that inhalation anesthesia perturbs the circadian rhythms requires further investigations. We assume that one of the reasons for these differences may be due to the tissue used for analysis. Most previous studies focused on the center of the circadian rhythm, the suprachiasmatic nucleus (Ueda et al., 2002; Panda et al., 2002). On the other hand, we used the whole brain as a target. The suprachiasmatic nucleus occupies an extremely small region of the whole brain. Therefore, the dilution of mRNA of the suprachiasmatic nucleus with mRNA of the whole brain might have affected the detection of the expression of the circadian genes mainly regulated in the suprachiasmatic nucleus. Furthermore, to obtain conclusive evidence for the association of anesthetic periods and the expression of circadian genes, future studies should scrutinize expression profiles for circadian genes at more multiple time points with a shorter interval than those used in this study. In order to further analyze the circadian gene expression, it would be useful to perform a non-microarray approach such as real-time PCR for the limited number of target genes as shown in this study.

In this study, we independently repeated the identical anesthetic experiment twice with rats. Clustering analysis shown in Fig. 1 exhibits that with the exception of the brain and kidney, in the other five organs smaller clusters are generated for each, which correspond to the two independent anesthetic experiments, reflecting experimental errors. Only the brain and kidney do not exhibit such smaller clusters that completely corresponded to the two independent experiments, indicating that in these two organs, experimental errors between the two experiments were smaller than the differences among individual rats and/or experimental conditions for anesthesia. These results clearly indicate that experimental errors among independent anesthetic experiments are not negligible and that one should be careful while drawing conclusions from a single experiment with animals under mildly different experimental conditions such as inhalation anesthesia. We successfully avoided highlighting genes that reflected the experimental errors by repeating the identical anesthetic experiments and conducting filtering operations for a combined gene expression data set. These findings provide experimental evidence that endorses the significance of repeating an independent experiment with animals under experimental conditions with mild differences and of data processing to reduce noises that reflect the differences among the repeated experiments.

As described above, our study demonstrates that the experimental errors observed between the independently repeated anesthetic experiments provided the second highest difference that follows the differences among the individual organs tested, which generated the most distinguishable clusters. This finding led us to use threshold-based approaches with strict cutoff values to extract genes in which expression was specifically affected by inhalation anesthesia and to avoid influence of the experimental errors and the differences among individual rats assigned for the identical conditions. These relatively strict analytical approaches may result in insufficient extraction of specifically affected genes, particularly for those in which expression was altered in a subtle manner. One of the analytical approaches that may enable us to obtain a greater number of genes specifically affected by inhalation anesthesia should be to apply lower thresholds in the filtering operation described in the Materials and methods for the data set compiled in this study. The approach may be effective to obtain as much information as possible from our primary data set. However, this would require additional confirmation for the individual values through non-microarray approaches.

We have provided a large and powerful data set for exploring the influence of inhalation anesthesia in rats. The entire data set will be available in a public database. The results presented here were derived from the data set by relatively conservative approaches due to the experimental differences greater than those expected prior to data analysis. Therefore, apart from conducting additional more fine-tuned experiments, another approach may be helpful for the further understanding of comprehensive influence of anesthesia by means of utilizing advanced statistical methods such as analysis of variance (ANOVA). Application of the more sophisticated approaches would enable those who use the data set to explore additional categories of genes that are modulated under anesthesia.

Acknowledgments

We thank K. Kon, S. Nakajima, and S. Nakamura for technical assistance.

Appendix A. Supplementary data

Supplementary data associated with this article can be found, in the online version, at doi:10.1016/j.gene.2005.03.022.

References

Ammon, S., Mayer, P., Riechert, U., Tischmeyer, H., Hollt, V., 2003. Microarray analysis of genes expressed in the frontal cortex of rats chronically treated with morphine and after naloxone precipitated withdrawal. Brain Res. Mol. Brain Res. 112, 113–125.

Baveja, R., Keller, S., Yokoyama, Y., Sonin, N., Clemens, M.G., Zhang, J.X., 2002. LPS-induced imbalanced expression of hepatic vascular stress genes in cirrhosis: possible mechanism of increased susceptibility to endotoxemia. Shock 17, 316–321.

Bhat, R.V., Worley, P.F., Cole, A.J., Baraban, J.M., 1992. Activation of the zinc finger encoding gene krox-20 in adult rat brain: comparison with zif268. Brain Res. Mol. Brain Res. 13, 263–266.

Brown Jr., B.R., Frink, E.J., 1993. The safety of sevoflurane in humans. Anesthesiology 79, 201–202.

Cannady, E.A., Dyer, C.A., Christian, P.J., Sipes, I.G., Hoyer, P.B., 2002. Expression and activity of microsomal epoxide hydrolase in follicles isolated from mouse ovaries. Toxicol. Sci. 68, 24–31.

Clarke, H., et al., 1997. Alpha-gluthathione *S*-transferase (alpha-GST) release, an early indicator of carbon tetrachloride hepatotoxicity in the rat. Hum. Exp. Toxicol. 16, 154–157.

Forrest, J.B., et al., 1990. Multicenter study of general anesthesia: I. Design and patient demography. Anesthesiology 72, 252–261.

Franks, N.P., Lieb, W.R., 1994. Molecular and cellular mechanisms of general anaesthesia. Nature 17, 607–614.

Freeman, W.M., et al., 2002. Changes in rat frontal cortex gene expression following chronic cocaine. Brain Res. Mol. Brain Res. 104, 11–20.

Gerhold, D., Lu, M., Xu, J., Austin, C., Caskey, C.T., Rushmore, T., 2001. Monitoring expression of genes involved in drug metabolism and toxicology using DNA microarrays. Physiol. Genomics 5, 161–170.

Gonzalez-Nicolini, V., McGinty, J.F., 2002. Gene expression profile from the striatum of amphetamine-treated rats: a cDNA array and in situ hybridization histochemical study. Gene Expr. Patterns 1, 193–198.

Harris, R.A., Mihic, S.J., Dildy-Mayfield, J.E., Machu, T.K., 1995. Actions of anesthetics on ligand-gated ion channels: role of receptor subunit composition. FASEB J. 9, 1454–1462.

Ito, E., et al., 2003. A tetraspanin-family protein, T-cell acute lymphoblastic leukemia-associated antigen 1, is induced by the Ewing's sarcoma–Wilms' tumor 1 fusion protein of desmoplastic small round-cell tumor. Am. J. Pathol. 163, 2165–2172.

Kobayashi, S., et al., 2004. Dynamic regulation of gene expression by the Flt-1 kinase and Matrigel in endothelial tubulogenesis. Genomics 84, 185–192.

Leloup, J.C., Goldbeter, A., 2003. Toward a detailed computational model for the mammalian circadian clock. Proc. Natl. Acad. Sci. U. S. A. 100, 7051–7056.

Levy, W.J., 1984. Clinical anaesthesia with isoflurane. A review of the multicentre study. Br. J. Anaesth. 56, 101S–112S.

Link, W., et al., 1995. Somatodendritic expression of an immediate early gene is regulated by synaptic activity. Proc. Natl. Acad. Sci. U. S. A. 92, 5734–5738.

Liu, C., Calogero, A., Ragona, G., Adamson, E., Mercola, D., 1996. EGR-1, the reluctant suppression factor: EGR-1 is known to function in the regulation of growth, differentiation, and also has significant tumor suppressor activity and a mechanism involving the induction of TGF-beta1 is postulated to account for this suppressor activity. Crit. Rev. Oncog. 7, 101–125.

Lu, A.Y., 1998. Drug-metabolism research challenges in the new millennium: individual variability in drug therapy and drug safety. Drug Metab. Dispos. 26, 1217–1222.

Lyons, T.J., Gasch, A.P., Gaither, L.A., Botstein, D., Brown, P.O., Eide, D.J., 2000. Genome-wide characterization of the Zap1p zinc-responsive regulon in yeast. Proc. Natl. Acad. Sci. U. S. A. 97, 7957–7962.

Mackenzie, P.I., et al., 1997. The UDP glycosyltransferase gene superfamily: recommended nomenclature update based on evolutionary divergence. Pharmacogenetics 7, 255–269.

Maruyama, K., Tsukada, T., Ohkura, N., Bandoh, S., Hosono, T., Yamaguchi, K., 1998. The NGFI-B subfamily of the nuclear receptor superfamily (review). Int. J. Oncol. 12, 1237–1243.

Panda, S., et al., 2002. Coordinated transcription of key pathways in the mouse by the circadian clock. Cell 109, 307–320.

Pei, Q., Zetterstrom, T.S., Sprakes, M., Tordera, R., Sharp, T., 2003. Antidepressant drug treatment induces Arc gene expression in the rat brain. Neuroscience 121, 975–982.

Ryabinin, A.E., Wang, Y.M., Bachtell, R.K., Kinney, A.E., Grubb, M.C., Mark, G.P., 2000. Cocaine- and alcohol-mediated expression of inducible transcription factors is blocked by pentobarbital anesthesia. Brain Res. 877, 251–261.

Schena, M., Shalon, D., Heller, R., Chai, A., Brown, P.O., Davis, R.W., 1996. Parallel human genome analysis: microarray-based expression monitoring of 1000 genes. Proc. Natl. Acad. Sci. U. S. A. 93, 10614–10619.

Snyder, M.J., Maddison, D.R., 1997. Molecular phylogeny of glutathione-*S*-transferases. DNA Cell Biol. 16, 1373–1384.

Sonin, N.V., Garcia-Pagan, J.C., Nakanishi, K., Zhang, J.X., Clemens, M.G., 1999. Patterns of vasoregulatory gene expression in the liver response to ischemia/reperfusion and endotoxemia. Shock 11, 175–179.

Storch, K.F., et al., 2002. Extensive and divergent circadian gene expression in liver and heart. Nature 417, 78–83.

Ueda, H.R., et al., 2002. Transcription factor response element for gene expression during circadian night. Nature 418, 534–539.

Yanagisawa, M., et al., 1988. A novel potent vasoconstrictor peptide produced by vascular endothelial cells. Nature 332, 411–415.